uc3m | Universidad Carlos III de Madrid

Bachelor's Degree in Aerospace Engineering
2016/2017

*Bachelor Thesis*

# Design and Thermal Analysis of a Space-Based Solar Power System

Eva Álvarez de Miguel

Tutor
Antonio Acosta Iborra

**Abstract**

This thesis is devoted to the thermal design of a space-based thermosolar power satellite with a nominal electric power of 1.2 MW. The aim of the thesis is to propose an alternative way of obtaining energy in space, and using it to power space vehicles. The satellite is designed to provide energy to the International Space Station, that now consumes 120 kW of energy, but the project assumes that this quantity would increase by a factor of 10 in the next decades.

In order to do the project, information about the use of solar energy and the evolution of the space-based solar power concept along time has been collected, and it is presented in the first chapters. It is also included an overview of the regulatory frame and the socio-economic context of the project.

The design of the power satellite is done by a separate analysis of each one of its components. As it is a central receiver system, the elements of the satellite can be divided into the power cycle, the receiver, the heliostat field and the accumulation system. In addition, the study of the orbit parameters is done for the design.

An analysis varying some relevant design parameters is done, and a comparison among the results is assessed so that the best possible choice is selected. The thesis ends with the main conclusions derived from the obtained results and some suggestions to improve their calculation.

# Contents

# List of Figures

# Chapter 1

# Introduction

The idea of this bachelor thesis arises from the concept of Space-Based Solar Power (SBSP), whose origin dates back to the late 1960's [1]. This concept is based on the utilization of a solar power satellite to catch solar radiation in the outer space, transform it into electricity and then beam it to the Earth in microwave or laser form.

Peter Glaser was the one who patented this idea in 1971 [2]. His goal was to get the maximum benefit from the large amount of energy radiated from the Sun. He though that by placing the sunlight conversion system beyond the atmosphere, any kind of attenuation produced by it, such as the presence of clouds or the filter produced by the composition of its different layers, could be eliminated. In addition, the night periods in which solar radiation does not reach the Earth surface would not be produced. In that way, the production of huge amounts of clean renewable energy together with a considerably reduction on the dependency of the limited fossil fuels could be achieved.

However, the present work does not deal with the design of a solar power satellite as the ones though originally when the idea of SBSP was born. The great majority of approaches proposed since Glaser's patent count with photovoltaic arrays for the solar-to-electric energy conversion and are focused on sending the electricity produced to its use on Earth. The power satellite to be designed in this thesis uses thermosolar conversion technology and its goal is to obtain electricity to power spacial vehicles, which eliminates the necessity to beam it to the Earth.

Thus, it is seen how the energetic problem on Earth, which was the main objective that Glaser had mind when he conceived the concept of SBSP satellite, is not solved by the thermosolar power satellite to be designed in the present project. Instead, it tries to define a possible alternative to the current ways of obtaining the energy used by spacial vehicles, so that more power can be produced and more complex missions are possible.

A specific section about the power consumption in space missions and the current power systems that are used is developed within this introductory chapter. In addition, the objectives, motivation and outline of the project are given to the reader in Sections 1.2 and 1.3.

## 1.1 Power consumption in space missions

In order to carry out a given space mission, it is essential to have access to the necessary power, so that all the systems implemented in the mission vehicle perform correctly its designed tasks. It is normal to think that not all space missions consume the same amount of power so, when designing the power system, the different needs of the specific mission must be taken into account.

The present section is subdivided in two parts. In the first one, the power required for some space mission is given, so that it is possible to have an idea of the amount of power consumed in space. The second part deals with the types of systems used to provide that required power. Most of the information included in the following paragraphs is extracted from Reference [3].

### 1.1.1 Power required for space missions.

Nowadays, there is a considerable diversification in the space missions objective and type. The first missions in the outer space were mostly dedicated to investigation and exploration, while at the present commercial and military missions have been added to the more scientific ones. Moreover, since the power systems have evolved, the complexity and duration of the missions have increased too.

Depending on the kind of mission, a different power system would be required. The selection of which power system to use is done by taking into account the amount of energy that it needs, how long the energy is needed and also the environment in which the vehicle will operate, in order to see if there is any available source in the surroundings from which power can be extracted.

Figure 1.1 shows how, depending on the mission, a different amount of power is needed. As seen, the missions which require more power are the space stations and the large communication satellites, being this some hundreds of kilowatts. Regarding the space stations, it can be appreciated the evolution of the technology during time, since Skylab, which was the first American space station, operated between 1973 and 1974 with less than 10 kW, while the International Space Station, which is currently operating since 1998, needs for its correct functioning 120 kW [4]. Thus, it is seen that as time has passed, more power is required for missions that are of the same type.

However, the amount of watts necessary to perform a mission is not the only requirement to design the power system, as previously mentioned. It is also important to know the duration of the mission, the objective that it has, the environment and path that it is going to follow, the possible energy sources that it may find in the surroundings, and many more features.

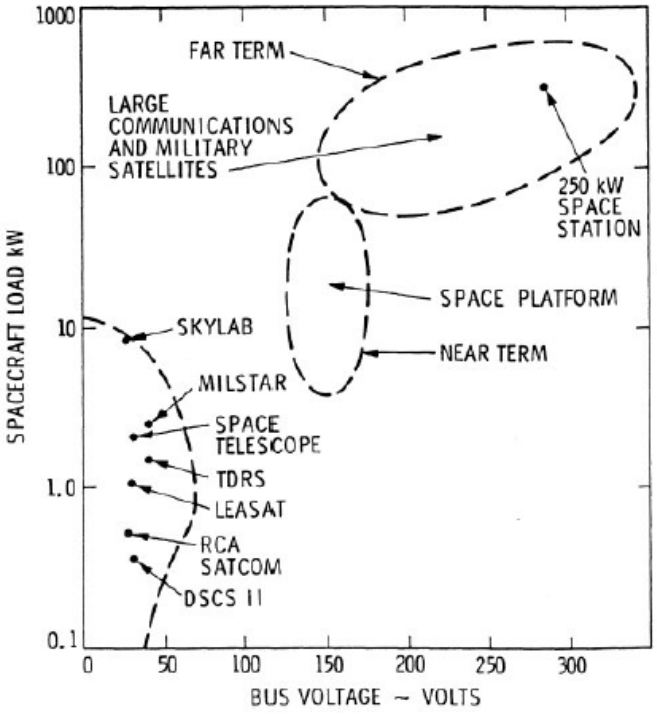


**Figure** 1.1: Power required for some missions.
**Source:** Ref. [3].

In the following section, the different power system solutions that have been used for each type of mission and how they have evolved during time are explained.

### 1.1.2 Power systems

At the beginning of the spacial era, primary batteries were used as the power system in the space missions. As seen in Figure 1.2, these batteries had a duration of just one or two days, so it was a strong limitation for the type of mission to be performed. Fuel cells were also used at the starting point of space missions, and could provide more watts and duration than the first batteries. However, a continuous flux of the chemical fuel (normally $H_2$) and oxygen or air is necessary for the correct operation of fuel cells, so its life is limited as well, in this case by the available amount of these elements in the space vehicle.

As the mission's objectives become more ambitious, new power systems were needed. The natural thing to do was thinking in the only source of energy that can be found in the outer space: the Sun. For this reason, photovoltaic panels

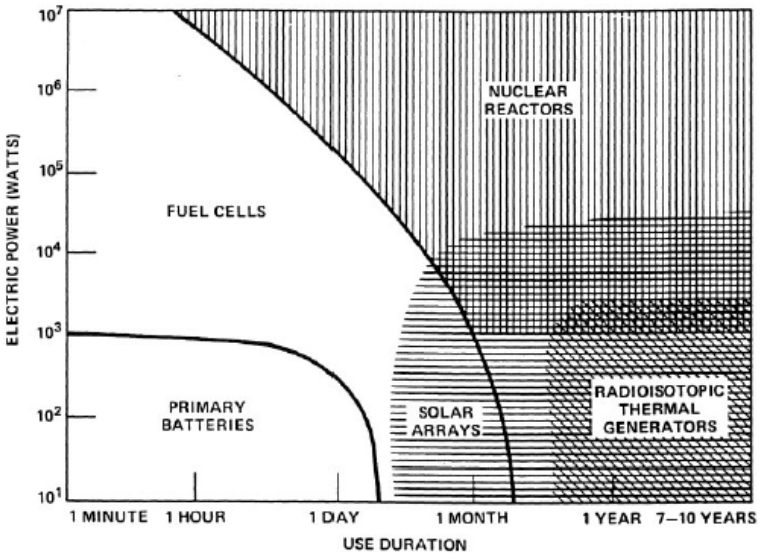


**Figure** 1.2: Regions of the power system to be used depending on the power required and the duration of the mission.
**Source:** Ref.[3].

were installed in the space vehicles and, with this new energy system, the duration of the mission was limited due to the structural degradation and not any more because of the lack of power. As seen in Figure 1.2, the photovoltaic cells do not provide as much power as other systems do. In fact, the conversion from solar energy to electricity is a bit inefficient in this type of cells.

However, when the space vehicle goes farther from the Sun, the solar cells are not as useful in order to obtain the required energy, because the radiation from the Sun that reaches the panels is weaker as the vehicle gets away. To solve this problem, the Radioisotope Thermoelectric Generator (RTG) was created. This power system is more efficient for missions in the outer solar system, and also allows to have a more compact power system compared with the photovoltaic cells.

The next step in the power system evolution was the space nuclear reactors. This power source was developed in the 1960's and, as seen in Figure 1.2, can produce great power and have a long duration. Besides, nuclear reactors are very compact, as for the case of the RTG.

Nowadays, new methods to provide power in space missions are being developed. It seems that future goals regarding space missions will require more power than the one that can be provide nowadays with the current power systems. For this reason, it is important to find solutions so that in the following decades power will not be an obstacle in the execution of space missions.

## 1.2 Motivation and objectives of the bachelor thesis

In this section, the motivation for the development of this bachelor thesis together with its objectives are explained in two separated paragraphs.

### 1.2.1 Motivation

As seen in Section 1.1, the procurement of power in space is essential for the achievement and evolution of space missions in the future.

The Sun is the greatest source of energy in space and using it as the principal source of power for a space vehicle is the best option if the mission takes place near Earth. Until now, solar radiation in space has been transformed into electricity by the use of photovoltaic panels and the obtained power has been enough for the correct functioning of the current vehicles.

However, in some years the space missions will evolve and more power will be needed, so that the inefficient conversion of sunlight into electricity produced by the PV cells will become a limitation for the implementation of modern missions. A solution to this problem is to use thermosolar conversion of sunlight into electricity instead of photovoltaic one, since it is more efficient in the obtention of high amounts of power. In addition, it is not easy to accumulate the electricity obtained from photovoltaic panels, especially if great amounts of energy are produced. This would be required to overcome the eclipse periods when sunlight is not available. In contrast, thermosolar conversion allows a relatively simple accumulation before it is transformed into electricity.

The present project deals with the thermal design of a solar thermal power satellite that will be used to give the required energy to the International Space Station or other station orbiting the Earth in a future. The ISS is nowadays one of the spatial vehicles which consumes more power. This power, which is around 120 kW [4], is of course provided by some photovoltaic cells. The idea is to size the new power system in order to give a power ten times greater than the one used today by the ISS, that turns to be 1.2 MW. This new power system is based in concentration thermosolar technology.

### 1.2.2 Objectives

The objectives of this project are enumerated in the following lines:

- To gather information about the evolution of the Space-Based Solar Power

concept since it was created at the end of the 1960's.

- To design the different components of a thermosolar power satellite of the central receiver tower type in order to produce a total electric power of 1.2 MW to achieve the possible future energy demand of the International Space Station or a similar spacial infrastructure.

- To develop a deeper analysis on the design of the receiver of the thermal satellite, which operates with molten sodium as working fluid, seeing the effects that are produced on its design when some relevant parameters are changed.

- To identify the possible improvements for the design proposed in this work so that further studies could be done based on this one.

It is necessary to have in mind that within this project only the thermal design of the solar power satellite is developed. Other important features for the design, as the structural analysis, are out of the scope of this thesis.

## 1.3 Outline

In this section, the different chapters that compose this project are described.

- **Chapter 1. Introduction**

  This is the present chapter that, as has been seen, contains a brief introduction about the power consumption in the space missions as well as the project motivation and objectives.

- **Chapter 2. Solar Energy**

  Chapter 2 deals with the solar energy and the different ways of using it. This chapter explains with more detail the classification and differences of the solar thermal power systems used in the present on Earth.

- **Chapter 3. Space-based Solar Power**

  Within the third chapter, the origin of the space-based solar power concept is explained together with its evolution along time and some interesting designs for the purpose of the one to be designed in the thesis.

- **Chapter 4. Regulatory frame and socio-economic environment**

  The regulations that need to be considered for the implementation of the power satellite designed in this project are explained in Chapter 4. In

addition, the social and economic impact are analysed.

- **Chapter 5. Design Methodology**

  In Chapter 5 it is explained how the design of each component of the thermosolar power satellite must be done. All the formulas to be used and the steps that are taken for the design are contained in the fifth chapter.

- **Chapter 6. Results**

  Following the instructions of Chapter 5, the design results can be shown, analysed and compared in Chapter 6. Both graphical and numerical results are present in this chapter.

- **Chapter 7. Conclusion**

  Finally, in Chapter 7, some conclusions extracted from the analysis of the results performed in Chapter 6 are summarized. In addition, some possible improvements of the project are suggested so that future research in the topic may be done.

In addition to the seven chapters just described, at the beginning of the project, before Chapter 1, a List of Contents and a List of Figures can be found so that the reader has direct access to each specific section or figure. Besides, the references used for the development of the thesis are enumerated at the end of the present report in the Bibliography.

# Chapter 2

# Solar Energy

The Solar System is composed of eight planets, including the Earth, all of them orbiting around the central star that gives its name: the Sun.

The Sun composition is: 73.46% hydrogen, 24.85% helium, 0.77% oxygen and the remaining 0.92% is carbon, iron, neon and other elements [5]. Nuclear fusion reactions happen at the core of the Sun, where atoms of hydrogen are pushed together due to the high pressure reached in this part of the star, creating helium and a great amount of energy. This energy is emitted to the space in form of light.

The solar energy that reaches the Earth can be transformed into electricity or thermal power to be used for human activities.

The thermal power system to be designed in this project is not going to be placed on Earth but instead will form a satellite orbiting the planet. However, it is important to have a general idea of how solar energy is used to obtain electricity on Earth and which are the main technological possibilities for the design of a solar thermal power system based on light concentration. In that way, it is possible to extrapolate the design followed on Earth to the one for the power satellite.

In the first section of this chapter, which is Section 2.1, a general overview of the available energy sources on Earth is explained in order to see the context in which solar energy is found. Then, Section 2.2 deals with the way in which this solar energy can be transformed into electricity. Finally, the types of solar thermal power systems are described in Section 2.3.

## 2.1 Energy Sources

In order to put the solar energy in context, a classification of the energy sources is done along this section.

The first division that comes to mind when talking about types of energy sources is whether they are renewable or not. The energy that can be obtained from non-renewable resources has a limit, that is, the rate at which oil or uranium is formed is lower than the consumption rate of the energy that can be get from them. In addition, a negative environmental impact is caused by the use of this kind of sources. On the other hand, renewable sources of energy are unlimited and clean.

The general classification of energy sources is the following:

- **Non-renewable energy sources:**
  - **Fossil fuels:** oil, coal and natural gas.
  - **Nuclear energy.**
- **Renewable energy sources:** solar, wind, biomass, tides, waves, geothermal, etc.

Although it may seem that the Sun is just one of a number or sources from which energy can be extracted, really it is the main source of energy of the Solar System, and most of the rest of energy resources do exist thanks to the action of the Sun. Fossil fuels were created thanks to the photosynthesis process in the first place, that is caused by the Sun, and the chemical reactions than happened afterwards due to high pressures and temperatures. Wind and tides are also formed due to the Sun, which is the responsible of the temperature differences that makes the air and water move [6].

## 2.2 Ways of using Solar Energy

From the previous section, it is clear the importance that the Sun has and the great amount of energy that it offers, in many forms. The topic of the present section, however, is the solar energy itself, in its primary form, and how it can be used and transformed.

Solar energy has been used during all human history, from drying food to conserve it for a longer period of time until the large solar power plants that produce electricity nowadays.

The first applications of solar energy mainly implied the use of the heat produced by the solar radiation directly to get the final objective. In that way, heat is used to dry food for preserving it by removing the humidity, or water can be desalinated so that it can be drunk. At the beginning, the amount of heat was the one given naturally by the sun, but then lenses and mirrors to concentrate the sun in a smaller area were developed, increasing the efficiency of these processes.

Another way of using the solar energy is to transform it into electricity, a more modern application that the previous one. In order to convert the solar energy into electricity, there are two options: transform it directly, with photovoltaic cells; or indirectly, transforming first the heat into mechanical energy and then creating electricity.

The scheme represented in Figure 2.1 summarizes these two different ways in which solar energy can be used: directly as heat or indirectly transforming it into electricity.

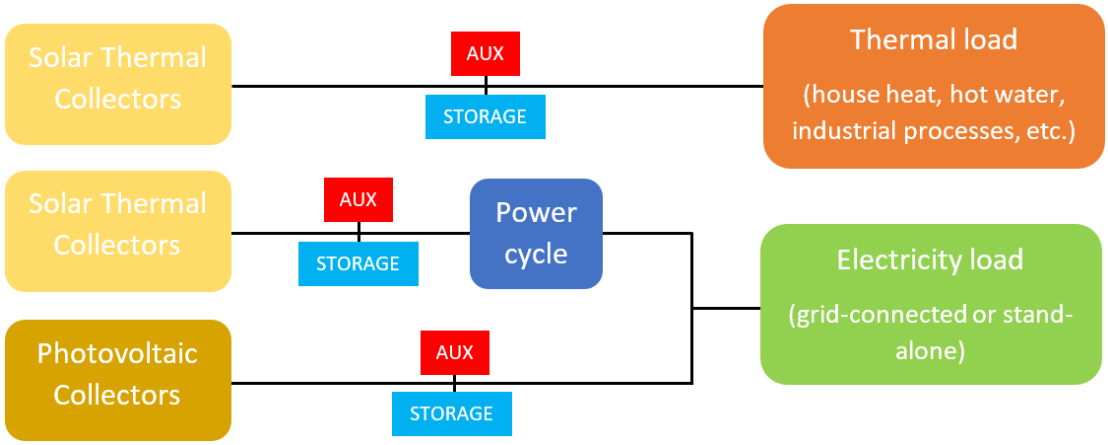


**Figure** 2.1: Types of solar power conversion.
**Source:** Ref. [5]

As it is observed, to transform the solar energy into electricity there are mainly two ways: solar thermal collectors and photovoltaic cells.

Photovoltaic (PV) cells are used to transform directly the solar energy into electric power. PV cells are formed by semiconductors, normally silicon. When photons from the Sun arrive to one side of the photovoltaic cell, an electron is taken from the valence shell, and is free to move through a conductor material to the other side of the cell, which is positively charged and thus attracts the electron [6]. This is how PV cells work and how electricity is created thanks to the photoelectric effect. The efficiency of this type of cell is not very high, around 13% [6]. Other problem of the photovoltaic cell is that when no sun light is present, it can not produce electricity, and for this reason batteries are needed if one can have a constant electricity source. The advantages of PV conversion system is that it is reliable and requires low maintenance, and, even though one cell produces a small power output, cells can be joint to form panels, which can be again joint to obtain the necessary power.

For the case of solar thermal collectors, a separate section will be used to explain in more detail the processes that takes place to transform the solar energy into electricity and the components that are present on them.

## 2.3 Solar Thermal Power Systems

Contrary to the photovoltaic cells, the solar thermal power systems transform the heat obtained from the sun to mechanical power first and then finally to electricity.

Figure 2.2 shows schematically the process followed by a solar thermal power system in order to pass from solar radiation to electric power.

First of all, the solar light is captured by the working fluid used in a collector, which transforms the radiation into heat. Then, it is optional to include an accumulation system so that it is possible to continue creating electricity while there is no sun light, i.e. during night or in a cloudy day. The hot working fluid is used to heat up the water in a boiler. In this way, the hot water moves a turbine which is part of the heat engine, thus transforming the heat into mechanical power, which is used to move a generator and obtain as an output electricity.

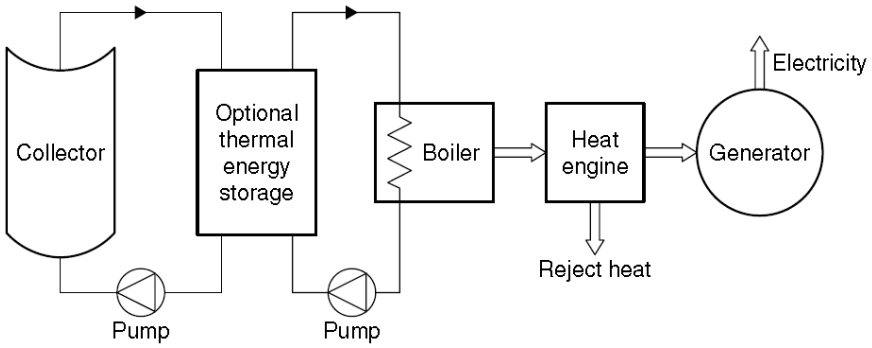


**Figure** 2.2: Scheme of the way a solar thermal conversion system works.
**Source:** Ref. [6]

It is possible to differentiate several types of solar thermal power systems. This classification is mainly based on the way the solar energy is collected. The three types of systems that are explained in this section are: parabolic trough collector system, parabolic dish system and power tower system.

### 2.3.1 Parabolic trough collector system

Parabolic trough collector system is the solar concentrating technology that has achieved the greatest maturity of all the possible ones. This kind of systems can reach temperatures of 400°C. The most important application of this concentrating system is the nine power plants in California that composed the Solar Electric Generating Systems (SEGS). Figure 2.3 shows a picture of one of these collectors, which belongs to the SEGS [6].

As it is seen in Figure 2.3, the parabolic trough collector is formed by a reflective material manufactured with parabolic shape. In the focal line of the parabola, a

straight tube that is used as the receiver is placed. A synthetic oil flows through the linear receiver, increasing its temperature as it passes thanks to the heat produced by the solar radiation that the parabolic reflectors concentrates. In this way, the solar radiation becomes useful heat. The hot oil then passes through a heat exchanger and heats up water to transform it into steam and, by means of a Rankine cycle, move a turbine. Here the heat has been transformed into mechanical energy, than finally is converted to electricity in a generator.

**Figure** 2.3: Parabolic trough collector system in California.
**Source:** www.solaripedia.com

A parabolic trough collector thermosolar system is formed by parallel lines of this type of collectors, that usually have a single-axis tracking system. The receiver tube is normally covered by a glass external tube so that less heat is lost by convection. The system can also count with a natural gas auxiliary subsystem that allows the production of electricity when the demand is higher than the produced just by the solar system [6].

### 2.3.2 Parabolic dish system

This solar thermal power system uses a parabolic dish reflector. In this case, the sun is reflected in the parabolic dish and concentrated to the focal point of the parabola where the receiver is placed. As it can be appreciated, it is very similar to the parabolic trough collector. Figure 2.4 shows the Eurodish collector.

In this case, the temperature achieved can be higher than 1500 °C, and it is the most effective collector system due to the fact that it has a double-axis tracking system which allows to point at every moment to towards the Sun. In addition, the type of power cycle related to this collector is the Stirling engine, in contrast to the Rankine cycle that is preferred for the parabolic trough ones [6].

As observed in Figure 2.4, the parabolic dish collector is by itself an independent

power system, but it can also be connected to greater collector system, being just a part of it.

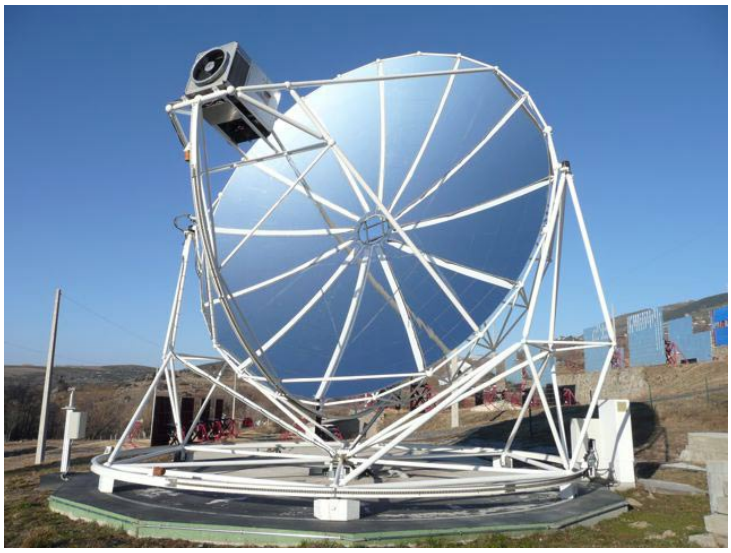

**Figure** 2.4: Parabolic dish reflector.
**Source:** www.promes.cnrs.fr

### 2.3.3 Power tower system

The power tower system follows a design quite different from the parabolic trough collector and parabolic dish systems. The main difference is that, whereas the two previously explained systems use independent concentration units that then can be grouped in order to increase the energy extracted, the power tower system has only one concentration point in the top or a central tower and all the collectors, in this case heliostats, are oriented to that point.

A thermosolar power plant of this type is composed essentially by the heliostat field, the central receiver at the top of the tower and a power cycle. Additionally, it may count with an accumulation system and some auxiliary power system. Figure 2.5 shows all the components in an scheme of a real power tower system.

Heliostats are basically mirrors that reflect the solar radiation to concentrate it in the central receiver. As there is only one point in which radiation is focused, this type of systems reach very high concentration ratios.

The central receiver is place in the top of the tower. There are different kinds of receiver that are used depending on the characteristics of the other components of the system. If a Rankine power cycle is used together with a large heliostat field, a cylindrical receiver is the best option. Other possibility is to choose a Brayton cycle for the heat engine, which needs higher temperatures for its correct operation. A better choice for this system would be a cavity receiver placed at a

higher tower with less heliostat density.

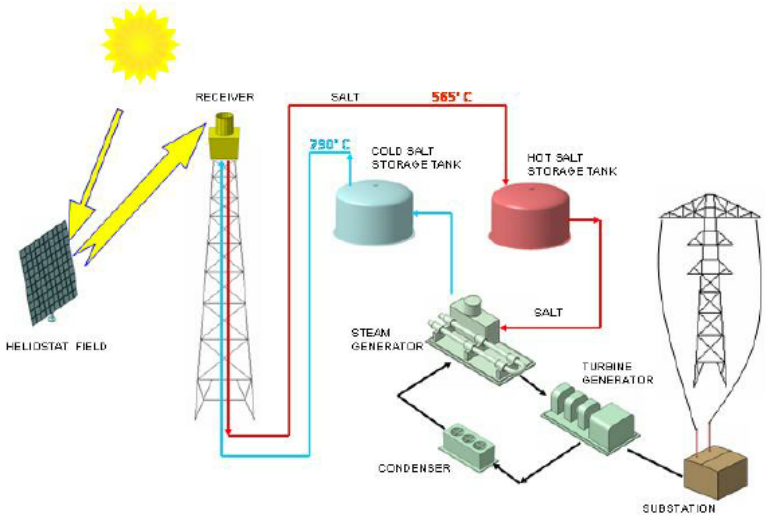


**Figure** 2.5: Working scheme of Gemasolar plant in Sevilla.
**Source:** Ref [7].

Figure 2.6 shows an example of this type of thermosolar systems. It corresponds to Gemasolar, located in Sevilla (Spain). It counts with a tower of 140 m and 2650 heliostat that are placed in a field of 185 hectares. Gemasolar generates 110 GWh in a year, which is translated into electricity for 25000 homes [7].

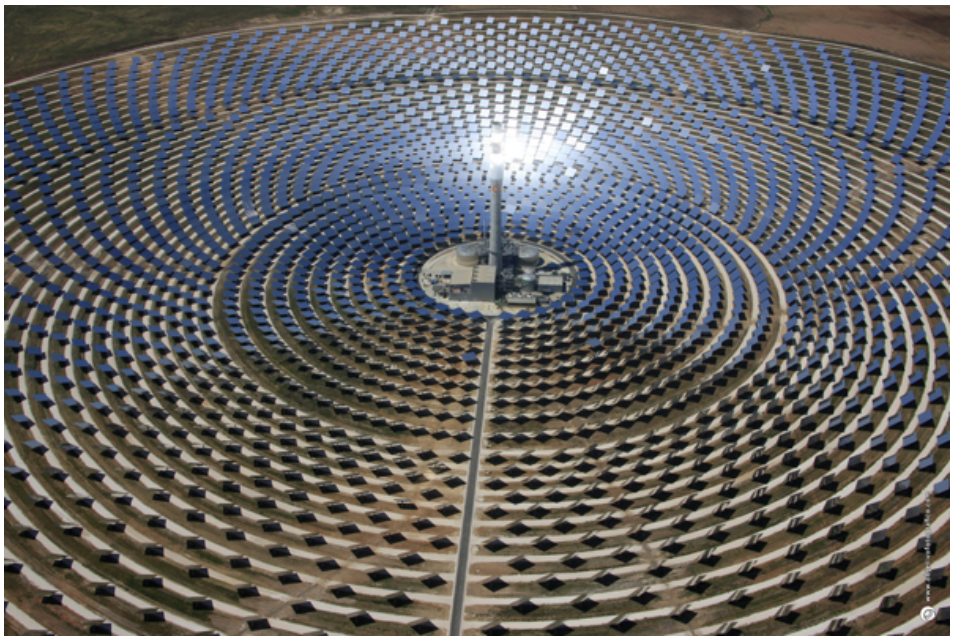

**Figure** 2.6: Gemasolar. Power tower system.
**Source:** www.torresolenergy.com

# Chapter 3

# Space-based Solar Power

> "The little, gleaming dots are huge masses of energy-filled matter. They are globes, some of them millions of miles in diameter [...]. They seem so tiny because they are incredibly far off.
>
> The dots to which our energy beams are directed, are nearer and much smaller. They are cold and hard and human beings like myself live upon their surfaces [...]. Our beams feed these worlds energy drawn from one of those huge incandescent globes that happens to be near us. We call that globe the Sun."
>
> *Isaac Asimov, 'Reason' (1941)*

The text that opens this section is extracted from the short story written by Isaac Asimov in 1941 called 'Reason' [8]. In the selected fragment, Powell explains to Cutie, the robot he has just built, how the station where they are works. The purpose of the station is to obtain energy from the radiation coming from the Sun and then beam it to different planets so that the humans living in them can use it.

In this story, Asimov for the first time talks about the space-based solar power concept, which probably he thought that could only be possible in his science fiction novels.

However, a lot of research on this topic had been done afterwards, and it is the purpose of this section to gather all the available information about it.

Space-based solar power concept consists on capturing solar energy in space, transform it into electricity and then beam it to the Earth for its use. All the process takes place in a satellite orbiting the Earth. In this way, there is no

atmospheric attenuation of the solar energy and the period of light in the cells is greater compared to an Earth-based solar power plant.

The vast majority of information about this topic is focused on two characteristics that are not the ones used for this project. The first one is the use of photovoltaic systems for the energy conversion and the second one, the fact that the energy is beamed to the Earth. The project idea is to design a solar thermal power plant orbiting the Earth and to use the obtained energy in the space.

Despite these two important differences, it is necessary to take a look to the studies done in the topic, just to see the global idea on which this work has been based.

## 3.1 Original SPS concept by Peter Glaser

Peter Glaser (1923-2014) was a scientist and engineer who contributed to the development of the aerospace and energy field. The space-based solar power concept was invented by him, and it was patented in 1971. Glaser introduced this concept by its definition of the SPS, which stands for Solar Power Satellite. He believed that this idea was the solution for the global energy problem, and defended it in articles and conferences [1].

This section aims to explain his idea of Solar Power Satellite, which was the reference point for subsequent configurations.

The SPS conceived by Glaser consisted on a satellite, or system of satellites, that could capture the solar radiation, transform it to microwave energy, and transmit it to some collectors placed on Earth for its use [2].

The inventor saw great advantages in the idea of using solar energy collected directly in the outer space. On the one hand, the Sun is an almost unlimited source of energy, and it is environment-friendly, as it does not produce any pollution. On the other hand, the fact that the energy is collected in a satellite, makes it possible to eliminate the problems of atmospheric attenuation, shadowing periods, dust deposition, etc.

Regarding the shadowing problem, it is true that, depending on the orbit followed by the satellite, there would be some periods in which the Earth itself would be positioned between the solar rays collector and the Sun. However, Glaser solved this problem by proposing the use of more than one satellite. In this way, he assured that his invention would provide energy without pause, because when one satellite was passing through the shadow produced by the Earth, another one would be receiving solar radiation and obtaining the required energy. Figure 3.1 represents the system configuration, where two geostationary satellites can be seen [2].

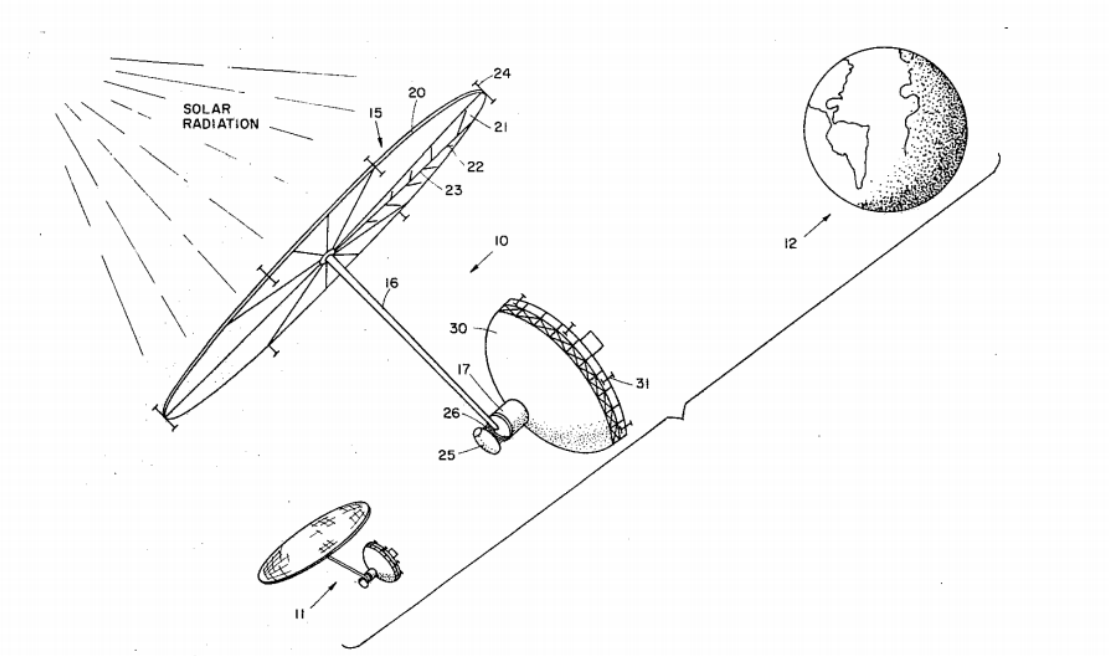


**Figure** 3.1: SPS Original Concept.
**Source:** Ref. [2]

The elements that Glaser described for his SPS are the following:

- **Solar energy collector and converter.** It is labelled as 15 in Figure 3.1. It consist on a large platform composed by several sectors that are responsible of capturing the solar energy and transform it into electric power. Glaser talks about photovoltaic cells, but any conversion system would be valid.

- **Support and link element:** Corresponds to number 16 in Figure 3.1. This part connects the collector with the antenna. Inside it, the cables through which the electricity travels are placed. As they need to carry a large amount of electric current, Glaser proposed superconducting ones.

- **Microwave Generator:** Necessary to convert DC electric current into microwave energy.

- **Antenna:** Number 30 in Figure 3.1. Component that beams the microwave energy to the Earth collector. It must be correctly oriented to reach the Earth-based collector with the minimum losses as possible.

- **Cooling system:** Necessary due to the high temperatures achieved in the satellite cables through which electricity travels. Glaser thought in a cryogenic refrigerator, that is placed in the housing labelled with number 17 in Figure 3.1.

- **Control Rockets:** Are placed in the solar energy collector as well as in the

antenna (24 and 31 at Figure 3.1). Are used in order to maintain the correct orientation of both elements. In the case of the solar collector, it must be always directed to the Sun, whereas the antenna must be pointing the Earth collector.

- **Earth microwave collector:** Consisting on a receiving antenna on a large area at the Earth so that the microwave power can be collected.

It must be pointed out that Glaser described the general components that the satellite must had, but the drawing in Figure 3.1 only represents a possible configuration. Other designs are also valid, as the one seen in Figure 3.2 that is more similar to a conventional satellite.

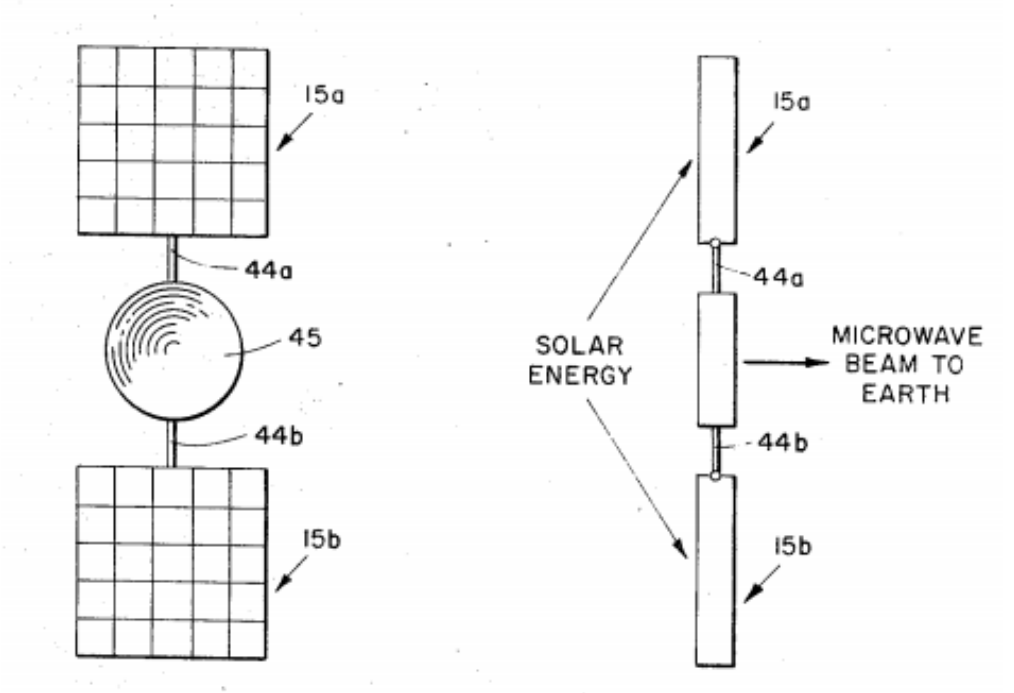


**Figure** 3.2: Another configuration of the SPS concept.
**Source:** Ref. [2]

## 3.2 SPS Reference System

As seen in the previous section, Peter Glaser was the inventor of the SPS concept. However, he did not enter into design details or the way of construction of the satellite. Based on Glaser's idea, some companies started to work on this concept and defined the so called SPS Reference System.

The NASA Centers together with the US Department of Energy (DOE) were the ones who combined the studies done by Boeing Aerospace Company (Dec 1976 - Dec 1977) and the analysis developed by Rockwell International (March

1977 - March 1978). With the data and information obtained from both research programs, the SPS Reference System was established [9].

The Reference System took the main idea of the concept of SPS developed by P. Glaser. However, in order to see the feasibility of the project, many factors needed to be taken into account, and the purpose of the reports written around the 80's about the Reference System was to close and define the details necessary to transform the initial idea into reality.

To do so, it was necessary to see the effects that the Solar Power Satellite would produce in the environment, the society and the economical impact, as well as the way in which each element of the satellite and the ground infrastructure was to be built, the transport of the pieces to the outer space and the cost to put it into the required orbit, etc.

Some of the technical aspects of the Reference System are summarized in the following lines. If the reader is interested in the complete research topics, please refer to [10], [9].

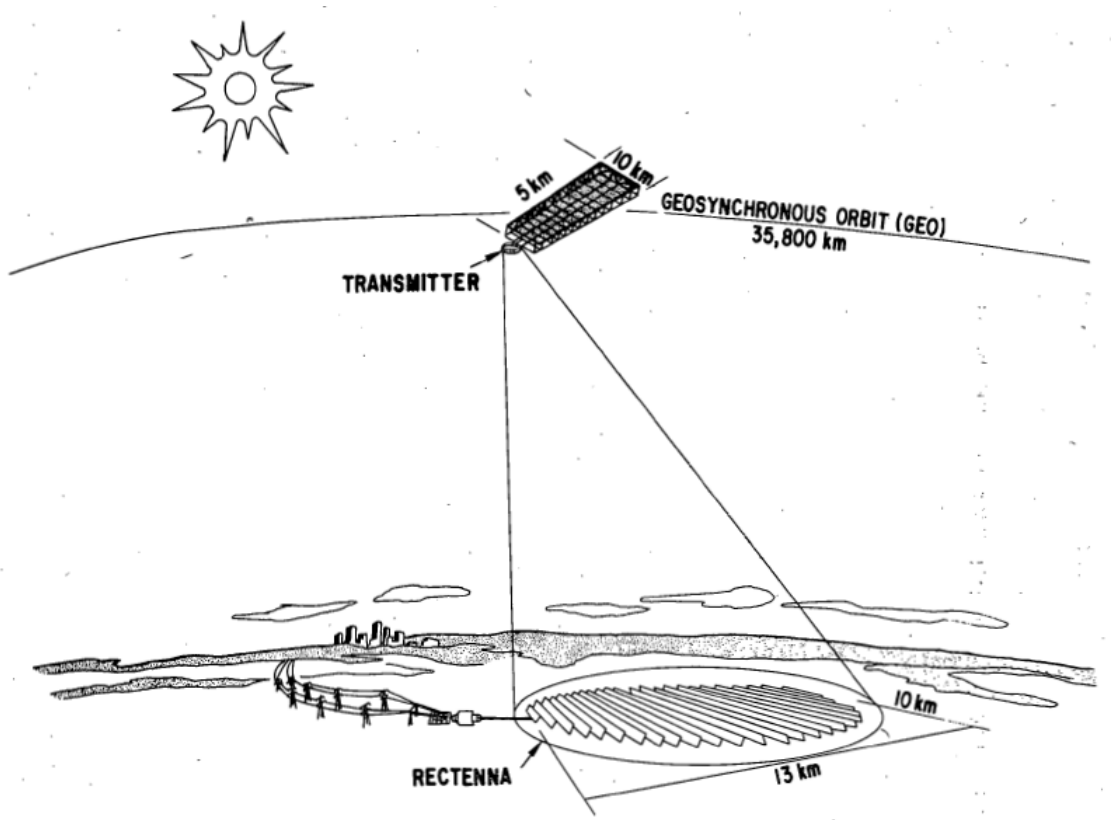


**Figure** 3.3: Solar Power Satellite Reference System Concept.
**Source:** Ref. [10]

Figure 3.3 shows schematically the SPS Reference System, with the most important

dimensions and the height of the selected orbit. Three basic elements can be appreciated, which are the rectangular solar array with its corresponding transmitter in the satellite, and the receiving antenna on the Earth. Notice that from now on, the antenna placed on ground to receive the microwave energy is called rectenna, in order to differentiate it from the antenna in the satellite, here called transmitter.

The most remarkable characteristic of the Reference System are the following:

- The system is sized to deliver 5 GW of DC current.
- The satellite is placed in a geosynchronous orbit.
- The structure is made of graphite composite.
- Photovoltaic solar cells are the ones used for the radiation-to-electrical energy conversion.
- To transmit the energy from the satellite to the rectenna placed on Earth, microwave radio frequency is used.

After the definition of the Reference system, some companies of different countries started to work in the development and the possibilities that the space-based solar power offered.

However, in the 80's, the interest of this topic waned due to the lack of technology and the possible damaging impact in the Earth environment caused by the microwaves from space, even though the great potential for the development of the idea in the future was unquestionable.

It was in the 90's when the concept patented by Peter Glaser was rescued and the 'Fresh Look' study developed. Then, at the beginning of the present century, it was finally concluded that its implementation was feasible.

## 3.3 Remarkable SPS concepts after the Reference System definition

The interest on space-based solar power, as previously mentioned, has two important peaks, in the 1970 and 2000. Studies about this concept were developed in different countries, such as the United States, Japan and recently Europe, as well as India and China, whose analysis are of less importance.

Among all the different possible architectures to implement the idea of the Solar Power Satellite, three main categories were identified by the International Academy

of Astronautics (IAA) in their report about this topic that was written in 2011 [11]. These three types of SPS are the updated 1979 SPS Reference, which is also known as the SPS Type I; the SPS Electric Laser Concepts, or SPS Type II; and finally, the SPS Type III is the SPS Sandwich and Related Concepts.

- **SPS Type I: Updated 1979 SPS Reference**

  The Type I SPS concept distinguished by the IAA in its Space Solar Power report has basically the components already explained in the Reference System, but some technical improvements are observed with respect to the configuration proposed in 1979. The main components are the large photovoltaic solar panels that are allowed to move with respect to three axes so that they are always pointing towards the sunlight, the microwave transmitter on the satellite and the receiver rectenna placed on Earth, which can be distinguished in Figure 3.4.

**Figure** 3.4: SPS Type I.
**Source:** Ref. [11].

- **SPS Type II: SPS Electric Laser Concepts**

  The SPS Electric Laser group differs from the previous one mainly on the way energy is transmitted from the satellite to the Earth, which is in this case done by laser instead of microwaves. Also PV platforms are used for the conversion or solar energy into electricity, just in the same way as Type I Space Power Satellites.

  The SPS Type II is depicted in Figure 3.5. As it is seen, two possible approaches inside this category are differentiated according to the photovoltaic platforms architecture. The first one, represented on the left, uses large PV platforms, as in the Type I configuration. The laser transmission devices are placed in the central structural component and are shared by all the cells. On the other hand, and represented in the right side

of Figure 3.5, it is possible to allocate individual PV elements forming a constellation, each one with its own laser transmitter.

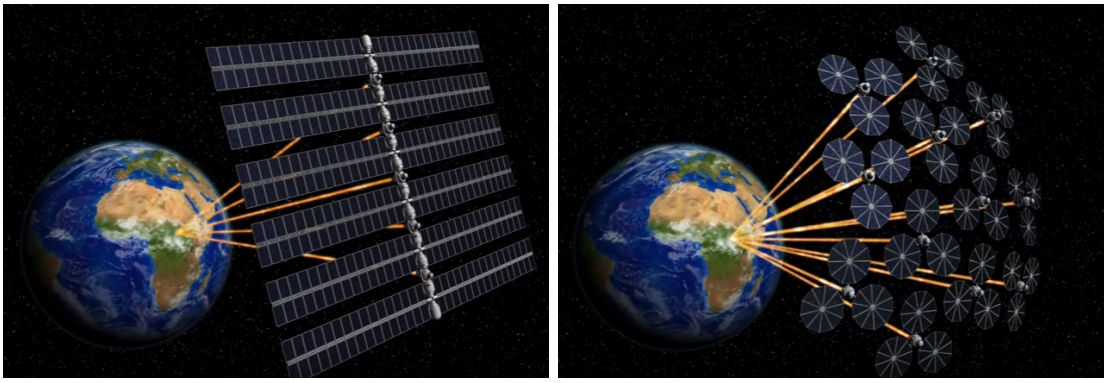

(a) Integrated platforms. (b) Contellation of individual laser platforms.

**Figure** 3.5: SPS Type II.
**Source:** Ref. [11].

- **SPS Type III: SPS Sandwich and Related Concepts**

  Finally, Type III SPS is similar to the Type I in the way energy is transmitted to Earth, which is by microwaves. However, the main characteristic of this type of satellites is the concentration mirrors that reflect the sunlight in a small photovoltaic array. As seen in Figure 3.6, the infrastructure of the SPS is symmetrically designed, having two mirror groups in the left and right extremes of the system and two little PV cells in the central part connected to the microwave generator and the transmission antenna that beams the energy to the rectenna on Earth.

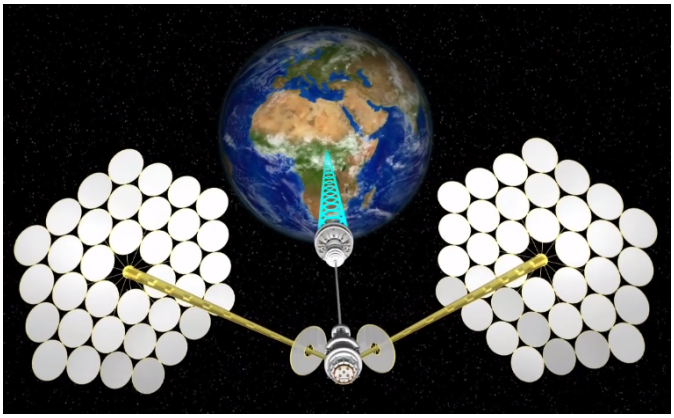

**Figure** 3.6: SPS Type III.
**Source:** Ref. [11].

The Sandwich SPS group is the most feasible one nowadays according to the IAA and it is of more interest as the previous ones for the current thesis since

it counts with a concentration technology, although the energy conversion is still photovoltaic.

In addition to the three types of SPS concepts defined by the IAA, diverse alternatives have been also proposed. Some of them are the Sun Tower SPS, the Integrated Symmetrical Concentrator, the lunar surface-based Solar Power, etc. However, it is not the purpose of this chapter to explain each of the different approaches that have been imagined since the Reference System, so if the reader is interested, a good overview of these configurations is contained in Reference [11].

Nonetheless, two extra architectures are included to finish with this chapter due to some interesting points that they have for the objective of this thesis.

The first one is the SPS-ALPHA Concept, developed by NASA in 2012 [12]. It can be considered as a Type III configuration, because it is composed by numerous mirrors that concentrate sunlight into a photovoltaic array than transforms it into electricity which is then transmitted to the Earth by its conversion in microwaves. However, the architecture can not be considered as a sandwich as the original Type III one. The remarkable feature about this concept is the distribution of the heliostats, which is very different to the previous ones. This shows how the structural limits in space are not as strong as on ground, so that any imaginable shape may be valid.

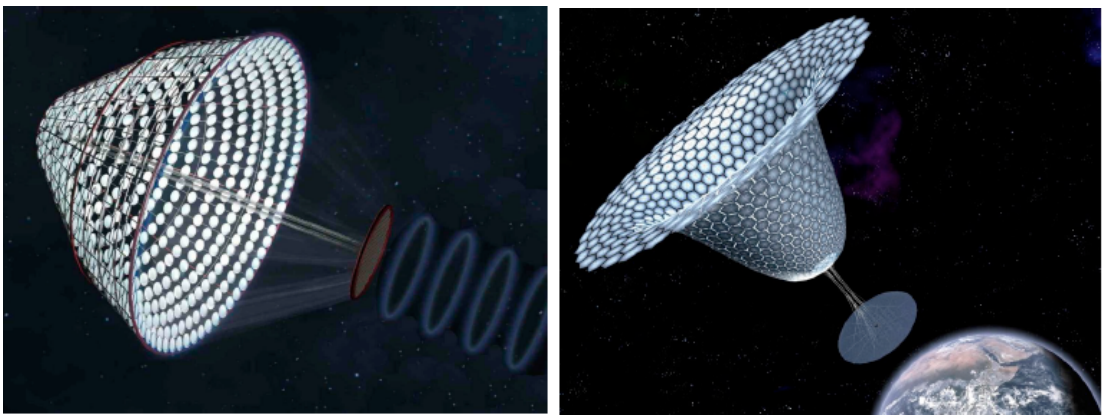

(a) Version 1. (b) Version 2.

**Figure** 3.7: SPS-ALPHA Concept by NASA.
**Source:** Ref. [12].

The second one is undoubtedly the most related approach to the system to be designed in this project. In all the SPS possibilities explained until now, the conversion of the solar radiation to electricity has been described by means of photovoltaic cells. The aim of the present thesis is to develop a thermosolar space-based power system, and an example of this kind of SPS was found. The concept was developed by Keith Henson, and his objective is to reduce the cost required to build previous SPS approaches. To get this cost reduction, Henson proposes solar-

thermal conversion instead of photovoltaic and new solutions for the transportation and construction of the complete satellite on the GEO orbit.

One of the advantages of using thermal conversion technology instead of PV is that the turbines do not degrade with the solar radiation as time passes. In addition, another favourable point for thermal power satellites is that they are three times more efficient than photovoltaic cells, so that less material is needed to obtain the same output power and cheaper is the mission to put all the elements in orbit [13].

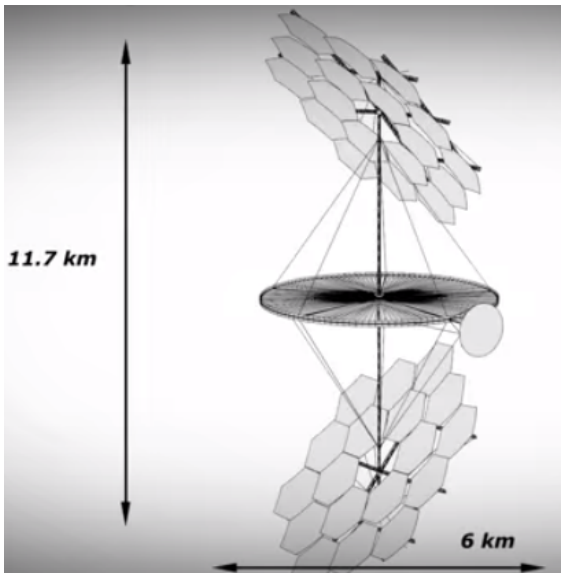


**Figure** 3.8: Solar-thermal SPS.
**Source:** Ref. [13].

The configuration of the thermal power satellite is depicted in Figure 3.8. As it is seen, it is composed by two heliostat groupings placed at the two extremes and a central disc structure. At one point in the perimeter of the disc, a circular surface perpendicular to the plane in which the central disc is placed is differentiated. This surface is the microwave transmitter, that must be positioned pointing to the Earth.

The disc-shaped assembly is formed by a radial module that is repeated for many angular positions until the complete circle is filled. The modular configuration is represented in Figure 3.9.

The elements of the power cycle necessary for the functioning of a thermal power system already explained in Section 2.3 are identified in Figure 3.9. The heliostats concentrate the sunlight in the boiler, heating up the working fluid. The superheated vapor moves the turbine and produces the required electricity by transforming this motion into electric energy using a generator that is not depicted in the image. Then, the heat must be rejected in a condenser, that for this case is a radiation tube, or a heat pipe, which will be the radiation system used also for the analysis done in this thesis. This pattern is repeated around the central structural element that joins the heliostat groupings with the central disc, so many

boilers, turbines and radiation tubes are needed for the system. Notice that boiler and turbine are the smallest components of the power system, placed very closed to the centre, while the major area of the disc is occupied with the radiators.

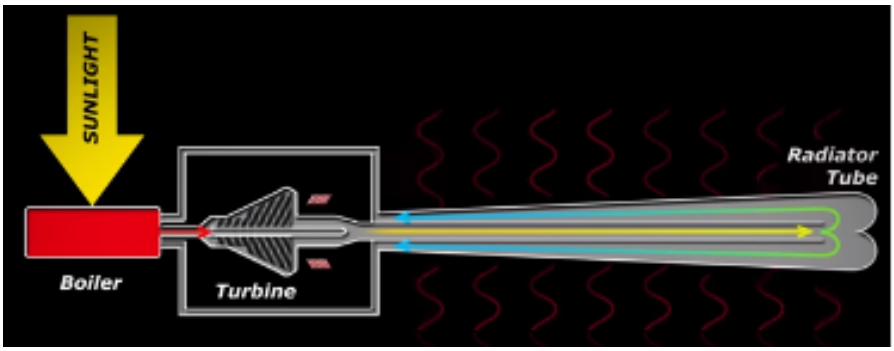


**Figure** 3.9: Solar-thermal SPS power system.
**Source:** Ref. [13].

## 3.4 Space-based solar power system to be designed in this project

After taking a look to some of the Solar Power Satellite systems that have been developed over the years since the Peter Glaser patent, it is necessary to clarify which are the characteristics for the system to be designed in this project.

The conversion system to obtain electricity from sunlight is a solar-thermal system by concentration, as already mentioned along this report, and the configuration used for that purpose among the ones explained in Section 2.3 is the central tower one. The idea is basically to reproduce the architecture of a central receiver thermosolar plant but instead of placing it on ground, make it orbit around Earth.

The main difference between the concepts already explained and the one to be developed in this project is the fact that the energy obtained in the satellite is not sent to the Earth either by microwave or laser. The idea is that the electricity produced in the satellite is used to power spatial vehicles instead of using it on Earth. In particular, the designed power satellite is though to power the International Space Station, so it is placed on the orbit followed by the ISS and connected to it by a cable to transmit the obtained electricity. A brief description of the ISS and the characteristics of the orbit that it follows is contained in the next paragraph, which is the end of this chapter.

### International Space Station

The ISS was developed by five partners: United States, Russia, Europe, Canada and Japan. Each one of the partners has contributed to the International State Station in a different manner.

NASA (US National Aeronautics and Space Administration) is the one who leads the ISS projects. However, the rest of the partners can send their own qualified astronauts to the station among other rights, and also are responsible of the maintenance of the components that each of them have provided to the ISS [4].

The ISS construction started in 1998, and its use have been approved at least until 2020 [3]. It is always inhabited and have been enlarged with more components over the years.

**Figure** 3.10: International Space Station
**Source:** www.estacionespacial.com

Figure 3.10 shows the International Space Station. As it can be seen, it has eight photovoltaic panels in each side to obtain energy for its correct operation. This energy is stored in some batteries, so that it can be used also when the ISS passes through the Earth shadow.

Regarding the orbit followed by the ISS, as the rest of space stations, it is a low Earth orbit, with an altitude approximately of 400 km. The International Space Station orbit has an inclination of 51.6º, as seen in Figure 3.11.

The inclination of 51.6º allows the ISS to pass above all the geographic points in Earth that are placed between latitudes 51.6º N and 51.6º S. This is due to the fact that the Earth rotates around itself, so when a revolution is completed by the space station, the Earth has move and a different geographic point is found

below it. The International Space Station performs fifteen and a half revolutions per day.

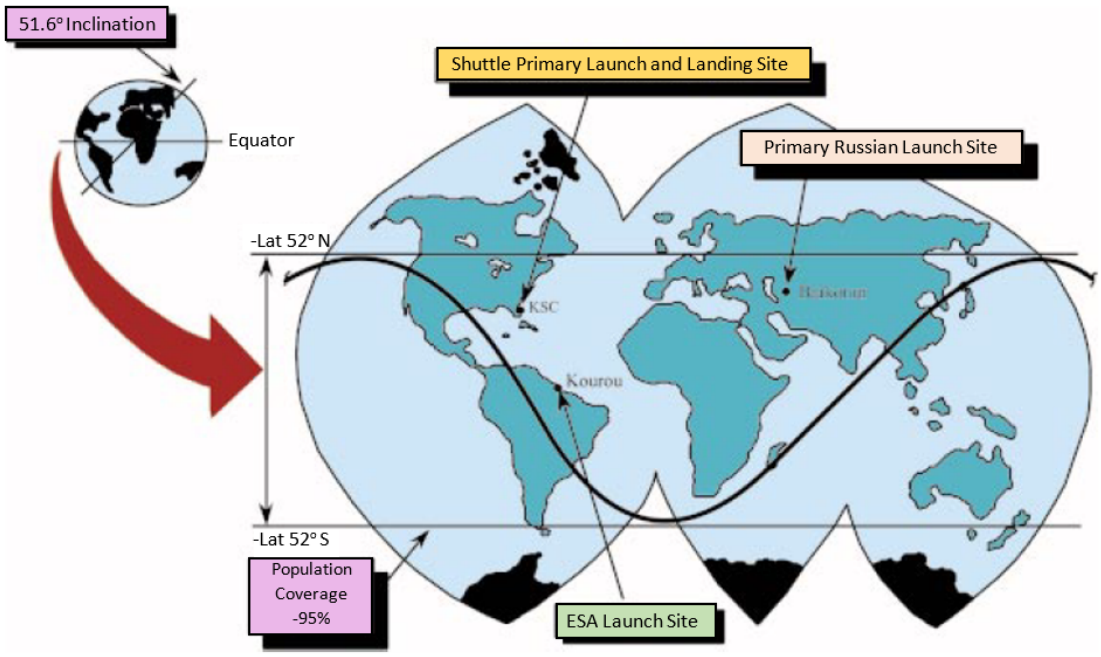


**Figure** 3.11: ISS orbit.
**Source:** Ref. [4].

# Chapter 4

# Regulatory frame and socio-economic context

Before entering into the design and analysis of the solar power satellite to be developed in this work, it is necessary to take a look into two important non-engineering aspects that must be considered in order to see the feasibility and impact of that infrastructure if it was finally built. These two aspects are the regulatory frame, contained in Section 4.1, and the social and economic impact, explained in Section 4.2.

## 4.1 Regulatory frame

The legal aspects behind the design and construction of the space-based solar power satellite to be developed in this project are contained in what is called the Space Law.

In the following paragraphs, the definition of Space Law and how it was created is explained. After that, a brief look into the main treaties in which space law is based is done and finally the most important aspects related with the solar power satellite are highlighted.

### 4.1.1 Introduction to Space Law

The Space Law emerges with the necessity of establishing some regulations and rules for the space activity. At the beginning, it was though that the same legal principle used to determine the airspace that each country owns was to be applied to the outer space. For the case of aircraft, it was determined that each nation have sovereignty of the airspace above its territory, adding to that piece of air 12

extra nautical miles from the country coasts to the sea. The sovereignty of the airspace, thus, was basically following the previous naval law.

However, some problem arose with the launch of the Soviet Union satellite Sputnik 1. This satellite was the first artificial satellite ever launched to space, and when it was put into orbit, the path followed by it passed over foreign territories, including the United States. If the same concept as for the airspace was applied in this case, the Soviet Union would have violated the law because they have no permission to overflight what may have been considered as United State territory. However, an agreement between Soviet Union and the US was created and the fact that the space law must differ from the air law, accepted [14].

According to the United Nations Office for Outer Space Affairs (UNOOSA), which is the institution in charge of establishing an international peaceful used of the outer space based on cooperation among states, the Space Law is *"the body of law governing space-related activities"* [15]. UNOOSA has developed five main international treaties that constitute the basis of the Space Law, but other international and national agreements, rules and regulations do also belong to what is globally called Space Law.

It must be noticed that there are still a lot of aspects that are not regulated under the Space Law because this field is evolving each day and not all the aspects involved are being considered yet. Nevertheless, the fundamental pillars are established in the five principal international treaties and so, an explanation of each of them is done in the following paragraph.

### The Five International Treaties

The five international treaties concerning the Space Law that were created by UNOOSA have been ratified by most countries and were created in different years. All of them follow the statement of UNOOSA that says that the *"primary goals of space law are to ensure a rational, responsible approach to the exploration and use of outer space for the benefit and in the interests of all humankind"* [15].

In the next paragraphs, a short explanation of each of them is included.

1. **The Outer Space Treaty**

   The real name of this treaty is "The Treaty on Principles Governing the Activities of States in the Exploration and Use of Outer Space, including the Moon and Other Celestial Bodies". It is the most important treaty of the five principal ones and was established in 1967. The content of the Outer Space Treaty mainly deals with the use of space as a peaceful zone; any military bases, installations or weapons are forbidden.

2. **The Rescue Agreement**

   The Rescue Agreement is the short name given to "The Agreement on the Rescue of Astronauts, the Return of Astronauts and the Return of Objects Launched into Outer Space". It started having legal effect in 1968 and its title basically explains the most important parts of its content, which is nothing else that each party who ratified the agreement has to do whatever is on its hands to assist or rescue astronauts in space, as well as recover objects to be returned to Earth.

3. **The Liability Convention**

   Its long name is "The Convention on International Liability for Damage Caused by Space Objects". It is dated to the year 1972 and says that any launching party has to give a compensation for any damage that may be caused on the Earth surface or in any aircraft by its launching object, as well as if two satellites of space vehicles collide.

4. **The Registration Convention**

   The Registration Convention, or "The Convention on Registration of Objects Launched into Outer Space" establishes that for any launch, it must be registered the name of the states involved, a registration number for the launched object, the date and location of the launch, as well as the orbital parameters and the purpose of the object that was launched.

5. **The Moon Treaty**

   The complete name of the last treaty is "The Agreement Governing the Activities of States on the Moon and Other Celestial Bodies" and it basically establishes the application of the Outer Space Treaty to the Moon and other celestial bodies in the solar system.

### 4.1.2 Related aspects of the Space Law with the satellite to be designed in this project

Once that a general overview of the more basic concepts related to the Space Law has been explained, an idea of the regulatory frame that is applied to the solar power satellite to be designed in this project has been created.

It can be said that the satellite itself and the power obtained by the solar-to-electric transformation produced inside it can only be used for peaceful purposes according to the Outer Space Treaty. The Rescue Agreement also applies if any component of the satellite may be returned to Earth for any reason. In addition, it must be checked that the launch of the satellite elements does not produce any

damage in other objects on Earth or in space to avoid any kind of accident and, if it happens, the corresponding compensation must be paid. Finally, needless to say, the satellite must by correctly registered in the United Nations database.

All what has been said until now is just based on the five general agreements that compose the Space Law. However, and as said before, there are other more particular agreements and regulations that can be applied more specifically depending on the type of object to be launched and the mission it will perform.

As the objective of the space-based thermosolar power satellite to be designed in this thesis is to provide power to the International Space Station, it makes sense to think that the "International Space Station Agreement" must also apply to this satellite. The ISS Agreement mainly deals with the establishment of the NASA as the leader agency, so that it will coordinate all the needed procedures to the final implementation of the power satellite. In addition, this agreement further specifies the general aspects covered in the five main treaties, particularizing them to the International Space Station case.

## 4.2 Socio-economic context

For the analysis of the socio-economic context of this project implementation, two separate sections are needed. First of all, just to have an idea, the budget of the project is estimated. Then, the impact in the society and the economy due to the development of a space-based solar power as the one designed here is discussed.

### 4.2.1 Estimated project budget

One of the principal reasons why space-based solar power to be used in the Earth has not been implemented yet is that the price of the electricity coming from one of these satellites cannot compete with the current one produced on Earth.

The problem is that the vast majority of SBSP designs are intended for being placed on a GEO orbit, and the cost of lifting off all the components to that orbit is not cheap. In addition, the weight of photovoltaic components is greater than the one for thermal elements, so a reduce in the cost could be reached if a thermosolar satellite was implemented instead of a photovoltaic one.

As the present project does not enter into the detail of materials and weight of the satellite infrastructure, the budget estimation is based on the information provided by Reference [16], which corresponds to a paper written by Keith Henson titled *"Solving Economics, Energy, Carbon and Climate in a Single Project"* that contains an economical analysis trying to prove that space-based solar power systems can be profitable.

In order to estimate the total budget, the features that must be taken into account are the components and construction of the power satellite and the lift-off cost of all these elements to the corresponding orbit.

According to Henson, the parts of the satellite and its assembly would have a cost of about US$ 900/kW, which corresponds to around 753€/kW. On the other hand, lifting-off any element to LEO would cost just US$ 120/kg (approximately 100€/kg) if the Skylon spaceplane is used. Skylon is yet under development and its first flight is scheduled for 2025, but if this vehicle performed 10,000 flights per year as it is said in Reference [16], the already mentioned cost for lifting any freight to low Earth orbit would be possible.

There is just one number left to be approximated, which is the mass of all the parts of the satellite to be lifted-off by Skylon. Japanese studies have established that 7 kg/kW are used in the case of a photovoltaic space-based solar power system. However, for a thermal one, this figure could be reduced to 5 kg/kW.

Taking all this into consideration, and having in mind that the thermosolar power satellite to be designed in this project is sized to give 1.2 MW, the estimated total budget of its implementation is US$ 1,800,000 which is equivalent to 1,506,564€.

Again, it is important to have in mind that this is just a rough estimation based on Henson paper, and that the budget could be different if a deeper analysis would be done. Nevertheless, hopefully the number given in that paper matches approximately with the real ones.

### 4.2.2 Socio-economic impact

The socio-economic impact that would be produced by the solar power satellite designed in this thesis is not easy to determine.

The satellite by itself is used to provide the necessary power for a space station that consumes 1.2 MW. With this amount of energy, the activities that take place in the ISS could be improved and more experiments undertaken. The results of these experiments could have a direct impact in society or economy, but it is not possible to know the extent of that effect if the objective of these activities is not known.

Nevertheless, it cannot be denied that a socio-economic impact would be produced direct or indirectly with the implementation of this new way of energy production.

If the power satellite turns to work well, it may be possible to improve it. In the future, new solutions for sending the produced electricity to the Earth could be found, so this thermosolar satellite could be the first step for the achievement of the main goal of Peter Glaser when he first thought about the space-based solar

power concept: solve the energetic problem in Earth. This could have a positive environmental impact, and the economy would considerably change taking into account the great weight that the energy sector has on it.

In addition, the applications of the power satellite as it is defined in this project could be used not only to give power to the ISS, but also, in the future, to give electrical energy to any other space vehicle, functioning as some kind of spatial service station.

Regarding the budget previously estimated, it could be afforded by the international governments and public organizations that have been the ones who have pushed the spatial sector since the beginning. However, the private companies are increasingly showing interest on this area, and it could be a possibility that they took over the costs of the mission.

# Chapter 5

# Design Methodology

In Chapters 2 and 3, background information about solar energy and space-based solar power was given, so that the project could be situated in context. Several aspects concerning regulation and the socio-economic impact of the construction of a thermosolar power satellite were given in Chapter 4, which made it possible to understand the implications and restrictions that are present if a project like this one is finally implemented. Now, in this chapter, the details of the solar power satellite design are specifically explained.

As already mentioned in this report, the objective of the project is to develop the thermal design for a space-based thermosolar power satellite. Its energy would be used in space, in contrast to the original function given to this type of infrastructures that, as explained in Chapter 3, was sending it to its use on Earth.

The design of the satellite is divided in several steps, which correspond to each of the elements that compose it. Hence, the very first aspect to be addressed in this chapter is the definition of each one of these elements and how they are connected among them. This is covered in Section 5.1. After that, a general description of the design process is given in Section 5.2, so that a kind of outline is depicted for the reader.

Then, five more sections are contained within this chapter, each one devoted to the specific methodology that must be followed to achieved the design of each component of the entire system. As it will be seen lately, these sections are: Orbit selection, Power cycle design, Receiver design, Heliostat field layout and Accumulation system.

## 5.1 Thermosolar power satellite description

Before starting with the details of the design process itself, it is essential to define and have in mind the different components of the solar-thermal power system, as well as its global operation.

In Section 2.3, a general overview of how thermosolar power systems work and the different types that can be distinguished attending to the collector they use was explained. Now, in this section, the components of the solar thermal power system that is designed in the present project are specified.

Before beginning with the explanation, it must be clarified that the system that is chosen for the development of this project is the power tower system with the central receiver, which was introduced in Section 2.3.3. Once this is known, it is needed to define in more detail the elements that form part of it.

Figure 5.1 shows all the elements involved in the process of electricity production within the thermosolar power satellite of central tower receiver. The following paragraphs are just the explanation of this figure, stopping in each depicted element to know the role each one plays in the complete system.

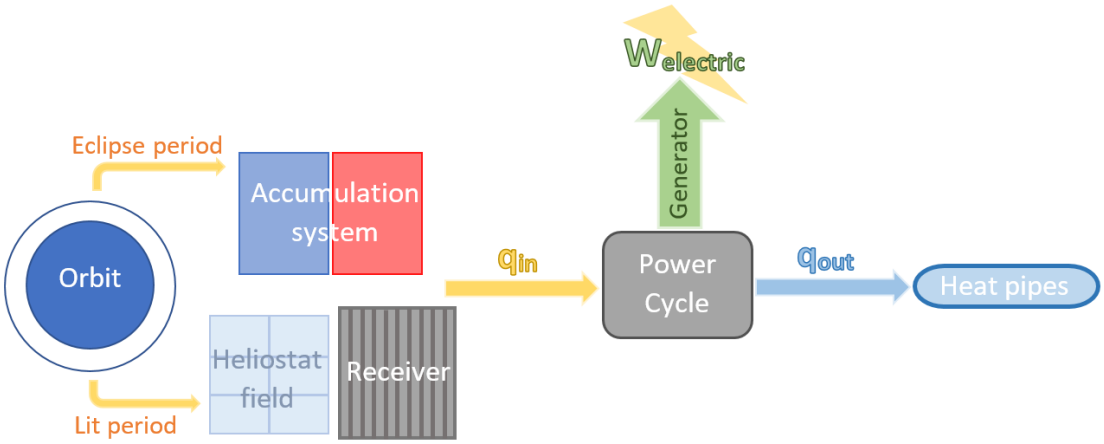


**Figure** 5.1: General overview of the power plant functioning.

The first feature that must be considered for the design of any type of solar power system is the place in which it is built, in order to know the time that Sun is available as the radiation source. In the case of this project, the location is not a very usual one, as it is orbiting the Earth. The advantage of having a thermosolar power satellite is that there are not clouds to hide the Sun, no atmospheric filter, and the position of the elements can be corrected with some attitude control systems so that Sun is always located in the zenith of the infrastructure. It is important to clarify that the attitude control system needs some energy in order to work and that it would be extracted from the one created with the power cycle. However, in the first design approximation calculated in this project, this amount of energy that the system must produce is neglected.

However, almost in every orbit around Earth, an eclipse period appears when the Earth is aligned between the Sun and the satellite, and this must be known and determined in order to size the system correctly. Thus, the thermosolar system works differently depending on the presence or lack of direct sunlight.

On the one hand, and as it can be seen following the lower arrow exiting the orbit symbol in Figure 5.1, when the satellite is moving in the lit side of the orbit, solar radiation reaches the heliostats. These mirrors reflect the solar rays and direct them towards the central receiver, concentrating the light on its surface and heating up the working fluid moving inside it. The type of receiver that is going to be used is a cylindrical one with liquid sodium as the working fluid. The selection of molten sodium among other possible fluids has been made because it is a molten metal that can stand high temperatures before evaporating. Besides, it is not very reactive with the materials of the receiver tubes, its risk of explosion is reduced since oxygen is not present in space and it can be directly used as the working fluid for the accumulation system.

On the other hand, while the satellite goes through the Earth shadow, which is represented following the upper arrow, the already heated fluid that is stored in the tanks of the accumulation system is used as the heat source.

As seen, following both paths the final result is a heated sodium, which then flows through the boiler of the power cycle producing an increase in the water temperature that flows through it. This heat source makes the functioning of the power cycle possible. The chosen power cycle is a simple Rankine one, whose details will be later explained in Section 5.4. This kind of cycle works well with the cylindrical receiver previously chosen.

Work is produced in the turbine of the Rankine cycle, and then it is transformed by a generator into electricity, which is the final objective of the power satellite. One important fact that must be taken into account is the way in which the heat is removed from the power cycle in the condenser. As the environment in which the power plant is working is the outer space, the only way to transfer the heat to the surroundings is by radiation. For that purpose, heat pipes are used, which will be explained in more detail in Section 5.4.3.

Another design consideration is the way in which the elements are going to be placed and attached among them. In Figure 2.6, the disposition of the elements corresponding to a common power tower system was shown. In the middle of the heliostat field, the tower with the receiver at the top is found. Next to the tower, and placed on the floor, the accumulation tanks and components of the power cycle are located. For simplicity, a similar distribution is used in this project, but instead of having the floor, all the elements would be attached with a truss structure. This distribution could be optimized for example by placing the heliostats in similar shapes to the ones shown previously in Figure 3.7.

## 5.2 General overview of the design process

Before explaining the calculations to be done, the sequence of the steps that are taken for the design need to be explained, so that the project can be followed more easily.

1. **Orbit selection:** This is the first step of the process. Knowing the orbit parameters, the lit and eclipse periods that the satellite experiences travelling through the orbit can be calculated, and thus, it is possible to size the accumulation system. In addition, with the selected orbit, an estimation of the receiver surrounding temperature can be obtained, which is a needed parameter for the receiver design.

2. **Power Cycle:** Having as main input the electric power to be delivered by the thermosolar satellite, the first step of the system design itself is to solve the power cycle, which in this case is a regular Rankine cycle with water as working fluid. From the power cycle solution it is possible to get two important outputs. The first one is the heat that must enter through the boiler to evaporate water. This heat is coming from the molten sodium, and it is an important parameter that will determine the receiver design. The second output is the heat that the condenser of the Rankine cycle must reject to the environment, and it will have an influence in the heat pipes dimensions.

3. **Receiver design:** Using as inputs the surrounding temperature computed with the orbit parameters and the heat that must enter in the power cycle, the receiver problem can be solved. This step of the project is the most complex one since, for solving the receiver problem, it is necessary to combine the equations that model the internal flow of sodium through it and also the external radiation that comes from the heliostat field. One of the most important outputs of this step is the radiation per unit of area that must be obtained in each point of the receiver so that the correct temperature rise of sodium is reached. This result will be used for the design of the heliostat field, which is the next step.

4. **Heliostat field layout:** As it has just been pointed out, the heliostat field is designed taking as input the output from the receiver problem. The radiation density computed in the previous step gives the number of mirrors that are needed, whereas the position of each of them is determined by a pattern extracted from the literature, which ensures that heliostats are not producing any shadow among them.

5. **Accumulation system:** The final step of the project is an estimation of the accumulation tanks dimensions. For this purpose, the lit and shadow periods computed in the very first step are needed together with some definitions from the receiver design.

As it is seen, the sequence to be follow for the system design is just following Figure 5.1 from right to left, except for the orbit selection step.

The next sections inside this chapter are the five steps that have just been explained.

## 5.3 Orbit selection

For a ground-based thermosolar power plant, the first design step to be taken is to select the location in which it is placed. This is essential for knowing the solar conditions of the area at which it will work, so that an efficient design can be developed.

For the case analysed in this project, the power system is orbiting the Earth, so the orbit parameters must be known for the same reason just explained regarding a ground-based power system. In particular, the eclipse period suffered by the heliostats when the Sun is hidden by the Earth and the effective temperature of the receiver surroundings are the required information to be extracted from the orbit parameters.

The eclipse period will be needed for knowing the total amount of energy that is produced in an entire orbit and the possible need of an accumulation system as well as its dimensions to counteract the shadowing period. Regarding the effective temperature of the surroundings, it is an important parameter for the receiver design.

In order to choose the orbit that the space-based solar plant is going to describe, it is essential to have in mind the users that will benefit from the power produced on it. Analysing the types of missions that are performed in space, it makes sense to use the produced energy to power the International Space Station. This seems to be a good option since the ISS is, nowadays, the space infrastructure that consumes more power.

In the present, the ISS is powered by 120 kW obtained from photovoltaic cells and accumulated in some batteries in order to have energy during the eclipse period [4]. However, the experiments and projects that astronauts perform in this station are more and more challenging each day, and available power could be a limiting factor for their activities in the next years. For this reason, this thesis considers that in the future the photovoltaic panels and batteries would not provide the necessary power for the station and that a thermal system, which can produce larger amounts of electricity in a more efficient way than photovoltaic cells, together with an accumulation system that stores more power than batteries would be a possible solution.

Another important factor for the design of a thermal power system established

on Earth, is the position of Sun along the hours of the day. This is used to know how heliostats must be oriented and how much solar radiation is reflected to the central receiver at each moment. However, for a space-based solar power plant, it is not necessary to analyse this factor, since its attitude can be modified and controlled using some sensors and thrusters so that the solar radiation comes always perpendicular to the plane in which the heliostat field is placed.

### 5.3.1 Eclipse period

An object orbiting the Earth will not receive sunlight at every point of its trajectory. When the Earth is positioned between that object and the Sun, it experiences an eclipse phase until the solar radiation can reach it again. In order to generate electricity in a thermosolar power plant, it is essential to be exposed to the solar rays, and when this is not the case, power must be created using accumulation systems or other resources.

For this reason, it is important to be aware of the eclipse period that the satellite experiences in the chosen orbit, just to know how much energy is obtained in a complete orbit and how to design an accumulation system in case of being necessary.

The formulas to compute the eclipse phase have been extracted from Reference [17].

From Equation (5.1) it is possible to compute the eclipse period of the orbit knowing some parameters.

$$T_e = \frac{T_o}{\pi} \arccos\left(\frac{\sqrt{2h+h^2}}{(1+h)\cos\beta}\right) \tag{5.1}$$

$T_o$ stands for the total orbit period, and it can be computed using Equation (5.2), in which $a$ refers to the semimajor axis of an elliptic orbit[1]; $h$ accounts for the relative altitude, defined in Equation (5.3) as the fraction of the orbit altitude from the Earth surface, H, divided by the radius of the Earth $R_E$; and finally $\beta$, which is the solar angle. All these parameters are better understood by looking at Figure 5.2, in which each of them is depicted.

$$T_o = 2\pi\sqrt{\frac{a^3}{GM_E}} \tag{5.2}$$

[1]Notice that for the case of the ISS, the orbit followed is almost circular, so $a$ would be the radius of the orbit.

$$h = \frac{H}{R_E} \tag{5.3}$$

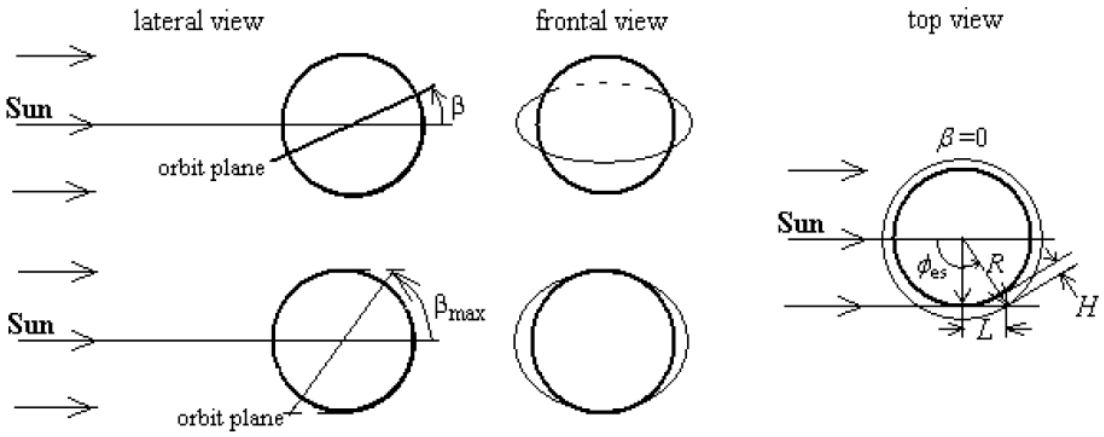


**Figure** 5.2: Orbit eclipse parameters.
**Source:** Ref. [17]

Table 5.1 summarizes the values of the constant parameters needed to solve Equations (5.1)-(5.3). In this table, $M_E$ is the Earth mass, G is the universal gravitational constant, $i_{ISS}$ accounts for the inclination of the ISS with respect to the equator and $\delta_E$ is the tilt angle of the Earth rotation axis with respect to the ecliptic.

| **H [km]** | **$M_E$ [kg]** | **$R_E$ [km]** | **G** $[m^3/kg \cdot s^2]$ | $i_{ISS}$ [º] | $\delta_E$ [º] |
|---|---|---|---|---|---|
| 400 | $6 \times 10^{24}$ | 6371 | $6.7 \times 10^{-11}$ | 51.6 | 23.5 |

**Table** 5.1: Orbit data.

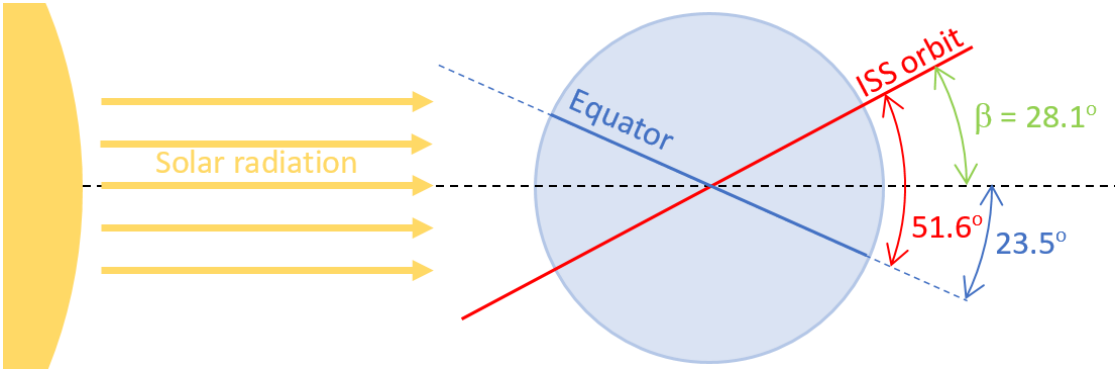


**Figure** 5.3: Solar angle $\beta$ definition.

The reader may have noticed that the angle of interest to compute $T_e$ is $\beta$, and its value is not given in Table 5.1. To calculate the solar angle it is only needed to

subtract the tilt angle of the Earth axis to the inclination angle of the ISS orbit, as represented schematically in Figure 5.3.

### 5.3.2 Effective receiver surrounding temperature

The other important data to be extracted from the selected orbit is, as previously said, the receiver temperature of the surroundings, i. e., the effective temperature in the space environment through which the power satellite orbits.

There are three main radiation sources that must be taken into account in the thermal control analysis of space vehicles. The first contribution comes directly from the solar radiation, whereas the other two are due to the presence of a celestial body near the vehicle. Any celestial body reflects part of the solar radiation that reaches it, which is known as the albedo, and it also emits infrared radiation due to its own temperature [18]. So, summing up, the three contributions that must be considered are the direct sunlight, the albedo and the IR emissions of a celestial body.

For the ISS orbit, the celestial body that needs to be taken into account for the albedo and the IR energy is the Earth. The typical values of each one of the contributions are stated in Table 5.2 [18].

| | |
|---|---|
| **Direct sunlight, $G_s$** | 1367 $W/m^2$ |
| **Earth albedo, $G_A$** | 410 $W/m^2$ |
| **Earth IR, $G_{IR}$** | 240 $W/m^2$ |

**Table** 5.2: Radiation sources that contributes to the space thermal environment of the ISS orbit.

Some clarifications of the numbers written in that table are needed:

- The given value for the direct sunlight is the solar constant. As the orbit of the Earth around the Sun is elliptic, the solar radiation varies along the year. At summer solstice, 1322 $W/m^2$ of sunlight reaches the Earth, while this value ascends to 1414 $W/m^2$ when the planet is at its closest position with respect to the Sun at winter. Therefore, the solar constant is just a mean value between the maximum and minimum ones.

- Regarding the value for the albedo, it is normally given by the percentage of the direct solar radiation that arrives to the corresponding celestial body. In the case of the Earth, the albedo accounts for the 30% of the solar constant, which gives the value stated in Table 5.2.

In order to calculate the effective temperature of the receiver surroundings, a method based on the one used for computing the effective temperature of a planet

is derived.

The procedure followed to calculate the effective temperature of a planet models it as a black body, so that the emitted radiation can be expressed with the Stefan-Boltzmann law, written in Equation (5.4)[2]. The energy per unit of area absorbed by the planet is $(1 - A)$ times the solar constant, being $A$ the albedo percentage. As the planet is assumed to be in equilibrium, the emitted energy (in watts) must be equal to the absorbed one, as expressed in Equation (5.5). Notice, that in that equation it is considered that the planet emits radiation in an area of $4\pi R^2$ whereas the absorption surface is just $\pi R^2$ [19].

$$E_b = \sigma T^4 \quad [W/m^2] \tag{5.4}$$

$$(1 - A)\, G_s \cdot \pi R^2 = \sigma T^4 \cdot 4\pi R^2 \tag{5.5}$$

Based on this method, a similar one is followed in this project to compute the effective temperature of the receiver surroundings. The receiver is modelled as a black body, whose panels are aligned with the solar rays. This is due to the fact that the plane in which heliostats are placed is oriented perpendicular to sunlight. Being aware that the cylindrical receiver is positioned perpendicular to that plane, it is demonstrated that panels are parallel to the solar rays. Thus, the direct radiation from the sun does not produce in the receiver surrounding temperature an effect as significant as if the rays came perpendicular to the panels. For this reason, a reducing factor must multiply the direct sunlight contribution. In the present thesis, a factor of 10% has been used, considering that at least a small fraction of the solar constant has an influence on the effective surrounding temperature.

On the other hand, the albedo and the IR emission from the Earth is multiplied by a factor that considers the heigh of the orbit. The 30% albedo assumes a source at 30 km from the Earth, for this reason, a correction factor is applied as written in Equation (5.6) [20].

$$F_a = \frac{(R_E + H)^2}{(R_E + 30\ km + H)^2} \tag{5.6}$$

The area that emits radiation is considered equal to the one for the energy absorption. This fact results in the cancellation of both area terms, getting Equation (5.7) as the final expression to compute $T_s$.

$$0.1 \times G_s + F_a \times G_A + F_a \times G_{IR} = \sigma T_s^4 \tag{5.7}$$

[2]Stefan-Boltzmann constant, $\sigma = 5.67 \times 10^{-8}\ W/K^4 \cdot m^2$

With this equation, the orbit calculations are done, and the next step of the process, which is the power cycle analysis, can start.

## 5.4 Power cycle

Once the orbit parameters are determined, it is possible to start with the design of the thermosolar power plant itself. The first step in this process is the power cycle.

As already mentioned, the power cycle chosen for the central receiver solar power system to be designed within this project is a Rankine cycle, which is a vapor power cycle that uses water as the working fluid. In particular, a basic Rankine cycle will be considered in this work because it is the simplest implementation of a vapor power cycle. Simplicity is a feature that is looking for to reduce construction and maintenance costs in space. In the Rankine cycle the water is subjected to different processes that will be explained more in detail in Section 5.4.1, and through them, electricity is created thanks to the produced work at the turbine that is then converted by means of a generator. Along the complete cycle, phase changes of water occur, the water being in liquid or vapor state depending on the cycle stage it is passing through.

The present section is split into three subsections. The first one deals with the general explanation of how the Rankine cycle works. The second, accounts for the procedure that is followed to solve the cycle and obtain the required information to continue with the next step of the design process. Finally, a third subsection contains the description of the condenser design.

### 5.4.1 The Rankine cycle

The basic Rankine cycle is composed by four different elements through which water passes: a pump, a boiler, a steam turbine and a condenser. The final goal of the cycle is to produce some work in the turbine shaft that will be used to move the generator which creates the electricity needed as final output of the entire power system. The work produced in the turbine is obtained by heating up the water in the boiler until it is transformed into vapor. This superheated vapor is the agent that moves the turbine blades producing mechanical work.

It can be said that the main input of the Rankine cycle is the heat at the boiler and the main output, the work on the steam turbine. However, a second output of it is the heat that exits through the condenser so that steam is again transformed into liquid water to start the cycle again, and a second input would be the work done by the pump to move water until the entrance of the boiler.

The cycle can be explained step by step by looking at Figure 5.4, which shows on the left the scheme of the basic Rankine cycle and on the right its Temperature-Entropy diagram.

1. At point 1 the water goes into the pump as a saturated liquid, as seen in the T-s diagram. Through the pump, an increase in pressure is achieved due to the work that it does, which, as said before, is an input to the cycle.

2. At the exit of the pump, at point 2, water enters the boiler and it is heated inside at constant pressure. For the case of a thermosolar system, the boiler corresponds to a heat exchanger, the hot fluid being the molten sodium heated by the solar radiation in the receiver.

3. Water exits the boiler in superheated vapor phase. Then it passes through the turbine in which heat is converted into work. This causes a pressure jump until reaching the same pressure as the one at point 1.

4. Finally, from point 4 to point 1, vapor is again transformed into saturated liquid water through the condenser by removing heat. The condenser is specially important considering that the thermosolar plant is located in the space, and its design will be described in Section 5.4.3.

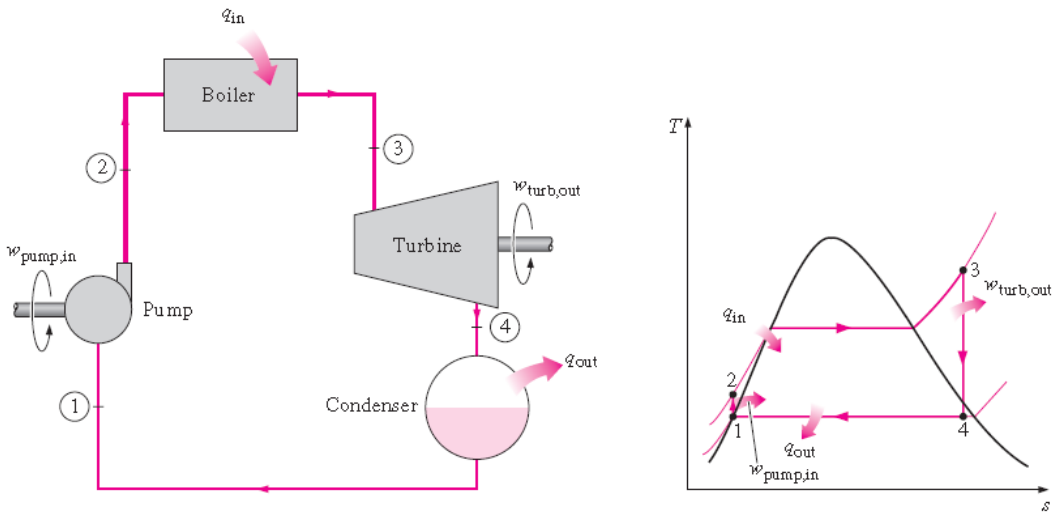


**Figure** 5.4: Basic Rankine cycle
**Source:** Ref. [21].

Paying attention to the T-s diagram, it can be noticed that processes through the pump and the turbine are assumed to be isentropic. This is because the represented graph describes the ideal Rankine cycle, but in real life, some inefficiencies must be considered, and are accounted in this project by the isentropic efficiencies that appears at Table 5.3. The same happens with the fact that pressure is maintained constant through the boiler and condenser. Some pressure drops happen but they are neglected in the calculations performed in the present work.

### 5.4.2 Procedure to solve the Rankine cycle

The principal output for the design that is extracted from the solution of the power cycle is the heat needed in the boiler so that the electric power for which the entire system is designed can be obtained.

For the case of this project, the desired electric power has been selected considering it to be ten times the current power used by the International Space Station, which is 120 kW. This gives as a result a design electric power of 1.2 MW as expressed in the first column of Table 5.3.

With the design power as the goal to be achieved, the heat that must be used in the boiler for heating up the water and turning it into steam can be calculated solving the basic Rankine cycle. To do so, several parameters need to be defined. These parameters are the temperature at the inlet of the turbine ($T_3$); the working pressures of the cycle, $p_b$ accounting for the pressure through the boiler and $p_c$ referring to the pressure thought the condenser; the isentropic efficiencies of the turbine and the pump; and the mechanical efficiency that is present in the conversion of mechanical energy from the turbine to electricity in the generator. Table 5.3 summarizes the chosen values.

| $W_{electric}$ [MW] | $T_3$ [°C] | $p_b$ [bar] | $p_c$ [bar] | $\eta_p$ [-] | $\eta_t$ [-] | $\eta_m$ [-] |
|---|---|---|---|---|---|---|
| 1.2 | 600 | 60 | 0.1 | 0.85 | 0.85 | 0.95 |

**Table** 5.3: Input parameters for the Rankine cycle.

Regarding the temperature at the inlet of the turbine, its value has been selected accounting for the limit that materials can stand currently without loosing their properties. Values for both pressures are typical ones for ground applications, which leads to common values for the isentropic efficiencies for the pump and turbine. These typical values for $p_b$ and $p_c$ allows to reduce the cost of design of components such as the vapor turbine, whose thermal and fluid dynamic behaviour for that pressure range is extensively reported in the specialized literature.

The mechanical efficiency used for the conversion of mechanical power to electricity has been set to 0.95. In Earth, the conversion process performed by generators has an efficiency very close to 1. However, for this case a smaller efficiency is used because, in space, friction is a problem due to the greater volatility of lubricants and the strong temperature changes at which mechanisms are subjected.

Once the input parameters are selected, it is possible to explain the procedure that must be followed to obtain the heat at the boiler.

The first step is to define the net power that must be obtained in the cycle. To do this, it is only necessary to solve Equation (5.8) for $W_{net}$, which just takes into account the mechanical inefficiencies.

$$W_{electric} = \eta_m W_{net} \ [MW] \tag{5.8}$$

Having the value of $W_{net}$, the solution of the Rankine cycle itself may be obtained. Through the boiler and the condenser, no work is done, because the pressure is maintained constant. The heat flux in both devices can be calculated following Equations (5.9) and (5.10), in which $q_{in}$ refers to the heat that enters in the boiler, $q_{out}$ to the one that leaves the condenser and $h$ to the enthalpy at the different points of the cycle, as represented in Figure 5.4. The enthalpy at each point is obtained knowing the temperature and/or pressure at them and using the water properties tables from the literature [21]. In order to get the solution for all the points, isentropic relations must be used.

$$q_{in} = h_3 - h_2 \quad [kJ/kg] \tag{5.9}$$

$$q_{out} = h_4 - h_1 \quad [kJ/kg] \tag{5.10}$$

With Equation (5.9) it is possible to get the heat at the boiler, which is the output needed for the power cycle to continue with the design. However, this heat is expressed in kJ/kg, so it must be multiplied by the water mass flow in order to change the units into kW.

The mass flow rate is obtained by computing the net work in kJ/kg, as stated in Equation (5.11), and then using Equation (5.12), in which the $W_{net}$ calculated from Equation (5.8) is introduced.

$$w_{net} = q_{in} - q_{out} \quad [kJ/kg] \tag{5.11}$$

$$\dot{m}_{water} = \frac{W_{net}}{w_{net}} \quad [kg/s] \tag{5.12}$$

Finally, using Equations (5.13) and (5.14), the required heat for warming up the water through the boiler is obtained, as well as the heat that must be radiated to the outer space in the condenser.

$$\dot{q}_b = \dot{q}_{in} = q_{in} \cdot \dot{m}_{water} \quad [kW] \tag{5.13}$$

$$\dot{q}_c = \dot{q}_{out} = q_{out} \cdot \dot{m}_{water} \quad [kW] \tag{5.14}$$

Also an important parameter for the Rankine cycle is the thermal efficiency, which is computed using Equation(5.15).

$$\eta_{th} = \frac{w_{net}}{q_{in}} = 1 - \frac{q_{out}}{q_{in}} \tag{5.15}$$

This efficiency will be used later for the accumulation system design and to see the global performance of the entire power plant.

### 5.4.3 Condenser design

The task of the condenser is to eliminate sufficient heat so that the steam that exits the turbine can be transformed into saturated liquid water at point 1 of the cycle (see Figure 5.4). As it is seen in the T-s diagram, temperature through the condenser remains constant, so the heat extracted is just the one required for the phase change.

All the removed heat from the condenser, $q_{out}$, must be transferred to the ambient, which in this case is the vacuum of the outer space.

In a condenser on Earth, it is easier to extract all that heat to the ambient because it can be transferred by convection, conduction and radiation. However, in vacuum the only way of transferring heat is by radiation.

The devices that have been selected to perform this task in this solar power satellite are heat pipes. In this section, a general description of the way heat pipes work is included. However, it is not covered the specific design of the heat pipes for its use in the thermosolar power satellite developed in this project.

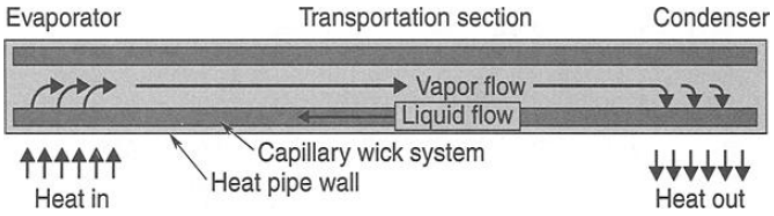


**Figure** 5.5: Heat pipe scheme.
**Source:** Ref. [18].

A scheme of the heat pipe operation is shown in Figure 5.5. Inside the heat pipe, there is a working fluid, that is present both in liquid and vapor state. The liquid remains at the wick, and the vapor is contained in the central part of the pipe. Both phases of the fluid remain at the saturation state. When some heat is added in the evaporator section, the fluid in liquid phase starts evaporating. This produces

a rise in the vapor pressure and thus a vapor flow towards the other extreme of the pipe, where the condenser is located. Due to the lower temperatures at the condenser end, heat is rejected and the fluid is transformed back into liquid.

Regarding the working fluids that are used for heat pipes, they are very different from each others and a specific one is used depending on their boiling, melting and critical temperature. Some examples of these fluids are given in Reference [18] together with their main three temperatures. They can be elements such as hydrogen or oxygen; or metals like sodium or lithium; or more complex molecules as methanol or ammonia.

For the Rankine cycle design, when water vapor exits the turbine, it transfers all the heat it has to the refrigerating fluid inside the heat pipes. Thus, the power cycle water becomes liquid before entering in the pump. On the other hand, the refrigerated fluid radiates all the heat to the outer space, following the heat pipe cycle already explained.

In is important to include in the design a kind of shell which maintains the heat pipes in a permanent shadow, so that Sun would not heat up the wall of the heat pipe. Also, it is possible to add some fins to the condenser section of the pipe, in which the vapor is transformed to liquid and heat is rejected, just to increase the contact area and facilitate the process.

## 5.5 Receiver design

As explained in Section 5.4.1, water passing through the boiler in the Rankine cycle is heated up until reaching superheated vapor state before entering in the steam turbine. The hot source that makes this heating possible is a salt or, in the case of this project, molten sodium, that has previously passed through the receiver tubes absorbing the incoming heat by radiation reflected from the heliostat field. Figure 5.6 shows this process.

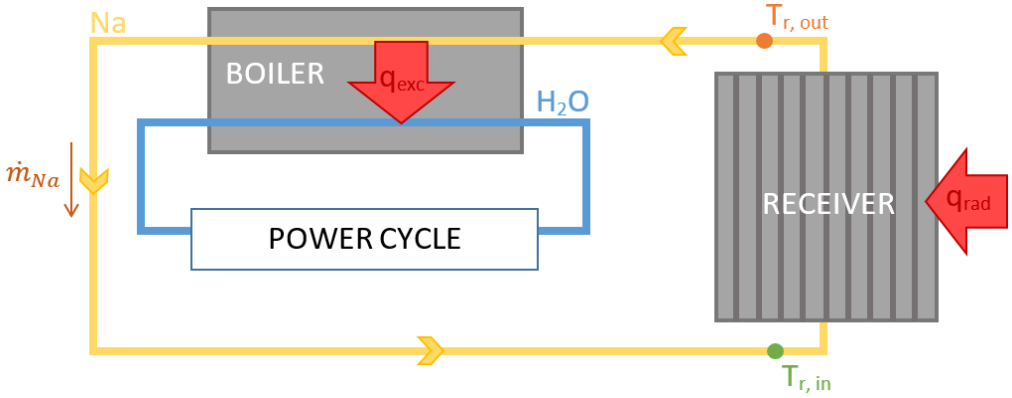


**Figure** 5.6: Heat exchange from liquid Na coming from the receiver and $H_2O$ in the power cycle.

The present section deals with the design of the receiver, obtaining its dimensions and the heat by radiation that must be provided by the heliostat field. This last feature would be the main input for the design of the field of heliostats, which is developed in Section 5.6.

It was already mentioned that the receiver chosen for the satellite design was a cylindrical one. However, until now, the elements forming the receiver have not been defined. A cylindrical receiver is composed by different panels, placed one next to the other until forming a cylinder. Several tubes are attached to each of these panels and, through them, the working fluid passes in order to be heated up. For the fluid to pass from one panel to the other, circular tubes called collectors are located in the two bases of the cylinder. The receiver geometry can be better appreciated in Figure 5.11, which is almost at the end of this section when dimensions are computed. Regarding the fluid flow between panels, it is depicted in Figure 5.10, also some pages below.

The first input in the receiver design is the value of $\dot{q}_{exc}$ represented in Figure 5.6, which is the heat that must be transferred from the liquid sodium to the Rankine cycle water. In Section 5.4.2, the procedure to compute $\dot{q}_b$ has been explained and, assuming that there is not any loss through the heat exchanger, $\dot{q}_{exc}$ would be exactly equal to $\dot{q}_b$.

Once the value of $\dot{q}_{exc}$ is established, it is possible to begin with the receiver design.

In order to compute the receiver dimensions, an internal and external analysis of the tubes that compose it is needed. Externally, the receiver is exposed to the incoming radiation concentrated on it by the action of the heliostat field. On the other hand, looking to the tubes internally, the flow of molten sodium is passing and being heated in order to reach the exit temperature $T_{r,out}$ from the inlet one $T_{r,in}$ (see Figure 5.6).

The outline of this section is the following: Section 5.5.1 deals with the external analysis of the receiver, which is the radiation circuit; along Section 5.5.2, the sodium flow inside the tubes is studied; Section 5.5.3 contains the expressions for computing the receiver dimensions; and, finally, Section 5.5.4 explains the way for computing the receiver performance.

### 5.5.1 Radiation circuit

As it has been said, the receiver is a cylinder formed by several panels, each panel composed by a number of tubes through which the working fluid is heated up. In order to analyse the radiation that heats up the receiver tubes, the radiation circuit formed by all the surfaces involved in the process must be defined and solved.

The first step is to identify the surfaces that must be considered for the radiation

circuit. On the one hand, it must be taken into account the receiver components, which are the tubes and the panels. Regarding the surface of the panels, it is idealized as a reradiating wall, which is characterized by emitting all the radiation that it receives from the other surfaces.

On the other hand, the surrounding environment in which the receiver works must be considered. It is at this point when the temperature of the surroundings $T_s$ that was defined in Section 5.3.2 enters into play. In addition, the irradiation coming from the heliostat field is considered, but the mirrors themselves are not taken as a surface of the circuit.

For studying the radiation circuit, it is necessary to model the cylinder as an infinite flat wall. Figure 5.7 shows the system representation needed for computing the values of the different view factors. The panel is thus considered as a flat wall, and is represented in grey and with the subindex $w$ (wall); tubes (subindex $t$) are coloured in orange; the blue colour is for the surroundings and green represents the heliostat field, both of them referred with the $s$ subindex as the value of their area and view factor is the same.

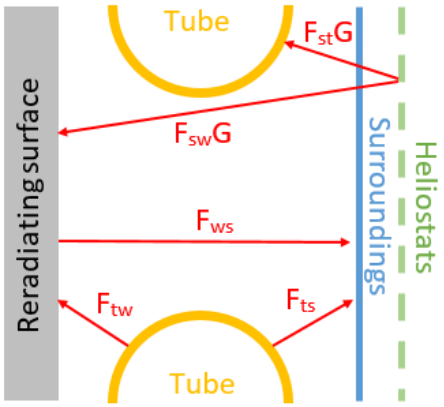


**Figure** 5.7: View factors representation for the radiation circuit in the receiver.

The radiation circuit is seen in Figure 5.8. Represented in orange it is possible to identify the radiation coming from the heliostat field to the tubes and panels of the receiver. The heat flux entering in the tubes is represented in red. The resistances (R), radiosities (J) and emissive powers (E) are all written using black colour.

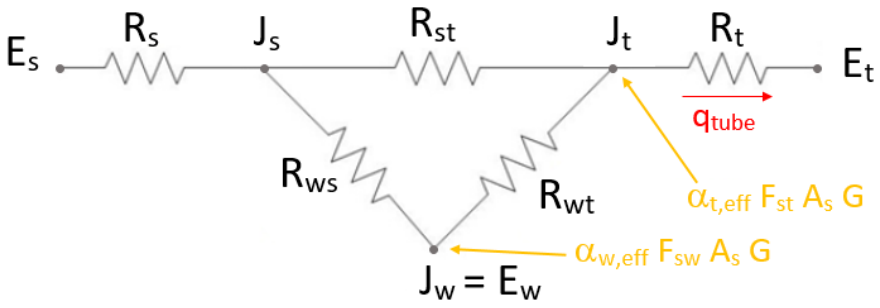


**Figure** 5.8: Radiation circuit in the receiver.

From the radiation circuit, four equations are extracted to solve the receiver problem. Equations (5.16), (5.17) and (5.18) are the ones corresponding to each of the three nodes seen in Figure 5.8. Equation (5.19), on the other hand, is the definition of the heat entering to the tube depicted with a red arrow in the same figure.

$$\frac{E_s - J_s}{R_s} = \frac{J_s - J_t}{R_{st}} + \frac{J_s - J_w}{R_{ws}} \tag{5.16}$$

$$\frac{J_s - J_w}{R_{ws}} = \frac{J_w - J_t}{R_{wt}} - \alpha_{w,eff} F_{sw} A_s G \tag{5.17}$$

$$\frac{J_s - J_t}{R_{st}} + \frac{J_w - J_t}{R_{wt}} = \frac{J_t - E_t}{R_t} - \alpha_{t,eff} F_{st} A_s G \tag{5.18}$$

$$\dot{q}_{tube} = \frac{J_t - E_t}{R_t} \tag{5.19}$$

In order to solve the system of equations (5.16)-(5.19), some known parameters and unknowns must be defined.

### Known parameters for the radiation circuit

The known parameters of the radiation circuit system of equations are explained and defined in these paragraphs. Basically, the known figures are the emissive power of the surroundings $E_s$, the radiation properties of each one of the surfaces, i.e. absorptivity and emissivity, the circuit resistances, the effective areas and view factors.

- **Emissive power of the surroundings, $E_s$**

  The surroundings emissive power is a known parameter. It depends mainly on the temperature $T_s$, that is calculated following the procedure explained in Section 5.3.2. The expression to compute this emissive power is the one written in Equation (5.20).

  $$E_s = \sigma T_s^4 \tag{5.20}$$

  In this equation, and as previously said in this project, $\sigma$ is the Stefan-Boltzmann constant, and it is equal to $5.67 \times 10^{-8}\ W/K^4 \cdot m^2$.

- **Radiation properties**

  Table 5.4 shows the emissivities and absorptivities for the tubes, panels and surroundings. Regarding the tubes and reradiating surface, the used values are the typical ones used when analysing a radiation circuit similar to the one developed in this project. For simplicity, variation of these properties with time as a function of time (due to the deterioration of the surfaces in space) will not be considered in this first study. For the surroundings, the absorptivity is not written since it is not necessary for the calculations, and the emissivity has been chosen considering both the outer space and the Earth.

| | **Tubes ($t$)** | **Reradiating wall ($w$)** | **Surroundings ($s$)** |
|---|---|---|---|
| **Absorptivity,** $\alpha_{eff}$ | 0.950 | 0.200 | - |
| **Emissivity,** $\epsilon$ | 0.850 | 0.200 | 0.885 |

**Table** 5.4: Radiation properties of the three surfaces involved in the circuit.

- **Circuit resistances**

  To compute the different resistances of the circuit, Equations from (5.21) to (5.22) must be used. In these formulas, $A$ accounts for area and $F$ for view factor. Both the areas and view factors are computed following the expressions explained in the next points.

$$R_s = \frac{1-\epsilon_s}{A_s\epsilon_s} \qquad R_t = \frac{1-\epsilon_t}{A_s\epsilon_t} \tag{5.21}$$

$$R_{ws} = \frac{1}{A_s F_{ws}} \qquad R_{st} = \frac{1}{A_s F_{st}} \qquad R_{wt} = \frac{1}{A_t F_{wt}} \tag{5.22}$$

- **Areas**

  The effective areas used to solve the radiation circuit are calculated with Equations (5.23) and (5.24). In these formulas, $s$ refers to the spacing between consecutive tubes, $d_{ext}$ to their external diameter and $L$ accounts for the length of the tube.

$$A_s = (s + d_{ext}) \times L \tag{5.23}$$

$$A_t = \pi d_{ext} \times L \tag{5.24}$$

- **View factors**

  In order to derive the expressions for the view factors, it is useful to take a look at Figure 5.7, in which the geometry of the problem is depicted.

  The key point for obtaining all the expressions for the view factors is to get the one for $F_{tw}$. For doing so, it is only necessary to go to Reference [22] in the bibliography and look for the formula that gives the view factor between an infinite plate and a row of cylinders. The expression found is written in Equation (5.25).

$$F_{wt} = 1 - \left[1 - \left(\frac{d_{ext}}{s + d_{ext}}\right)^2\right]^{1/2} + \left(\frac{d_{ext}}{s + d_{ext}}\right) \arctan\left[\left(\frac{(s + d_{ext})^2 - d_{ext}^2}{d_{ext}^2}\right)^{1/2}\right] \tag{5.25}$$

  After this is done, and giving a look at the equations where view factors are involved, it is only needed to find an expression for $F_{ws}$ and for $F_{st}$. Regarding the view factor between the surroundings and the tubes, it can be modelled as the one previously computed between the reradiating wall and the tubes, because the geometry is just the same. This fact is expressed in Equation (5.26).

$$F_{st} = F_{wt} \tag{5.26}$$

  For computing $F_{sw}$, a property of the view factors needs to be used. This property says that the sum of the view factors between a given surface and each one of the remaining surfaces involved is equal to one. This property is applied specifically for the reradiating wall in Equation (5.27). Notice that $F_{ww}$ is just zero because the panel do not interact with itself, as it does not have any curvature.

$$\sum_{j}^{Surfaces} F_{ij} = 1 \longrightarrow F_{ws} = 1 - F_{wt} - \cancel{F_{ww}} \tag{5.27}$$

### Unknowns to be solved in the radiation circuit

All the other parameters that have not been mentioned in the previous list, are the unknowns of the system of equations from (5.16) to (5.19). These unknowns are $J_s$, $J_w$, $J_t$, $q_{tube}$, $E_t$ and $G$.

As one can notice, there is a total of six unknowns, and just four equations. Therefore, in order to close the system and find a solution, two extra equations are needed, and those ones are found in the analysis of the liquid sodium flowing inside the receiver tubes, which is explained in the next section.

### 5.5.2 Liquid sodium flow through the receiver tubes

As said in the previous point, additional equations are needed to close the problem. To find those expressions, the flow of liquid sodium inside the tubes is analysed.

Figure 5.9 shows an scheme of the tube which will be helpful for understanding the next equations. In this scheme, $T_2$, $T_1$ and $T_t$ refer to the temperature of sodium at the exit of the tube, the inlet temperature of Na, and the temperature of the external surface of the tube, respectively. Dimensions of the cylindrical tube ($d_{ext}$, $d_{in}$ and L) are also represented, as well as the conduction coefficient of the tube, $k_t$, and the convective coefficient for sodium, $h_{Na}$.

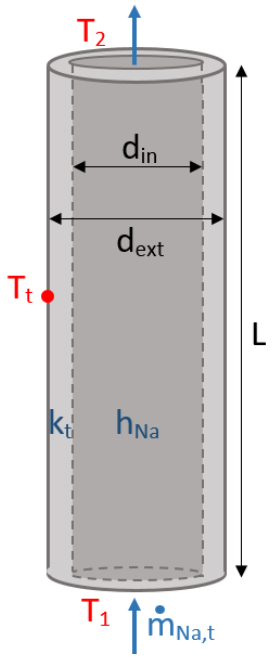


**Figure** 5.9: Liquid sodium through the receiver tube.

Temperatures $T_1$ and $T_2$ as well as the convective coefficient and mass flow rate, are defined later in this section. The length L is in principle an unknown, but the values of the diameters and conductivity of the tube are given by typical values in receivers of thermosolar central-receiver plants built on Earth.

Table 5.5 summarizes these values together with the space between tubes, that is also needed in the calculations. It must be noticed that the value for the thermal conductivity $k_t$ is the one corresponding to Inconel 600 allow, which is the material used for the tubes

| $\mathbf{d}_{in}$ [cm] | $\mathbf{d}_{ext}$ [cm] | $\mathbf{k}_t$ $[W/m \cdot K]$ | s [mm] |
|---|---|---|---|
| 1.88 | 2.67 | 25 | 2 |

**Table** 5.5: Tube known data.

The first equation to be considered is just the heat needed through the tube in order to pass from the temperature at the inlet to the one at the outlet. This expression is written in Equation (5.28), in which $\dot{m}_{Na,t}$ and $c_{p,Na}$ are, respectively, the mass flow rate and the specific heat capacity of sodium.

$$\dot{q}_{tube} = \dot{m}_{Na,t} \times c_{p,Na} \times (T_2 - T_1) \tag{5.28}$$

Finally, the second extra equation is related with the temperature at the surface of the tube. If the length L is not very large, it is possible to assume that $T_t$ is uniform along the tube, which implies that $T_t \approx \tilde{T}_t$, with $\tilde{T}_t$ being the mean temperature in the tube surface. Besides, changes of temperature along the angular direction in the pipe are present, so that $\tilde{T}_t$ refers to the mean temperature along the perimeter of the tube. Working with mean temperature reduces the spacial resolution of the calculations so that the maximum local temperature on the tubes is underpredicted. However, this will not compromise the design, since liquid sodium and the tube materials withstand temperatures greater than the ones selected in this work. The impact of working with mean temperature in the radiative heat transfer will be neglected as a first approximation.Taking into account this simplification of the problem, Equation (5.29) can be applied. Therefore, $\tilde{T}_t$ can be computed for given $T_1$ and $T_2$.

$$\frac{T_2 - \tilde{T}_t}{T_1 - \tilde{T}_t} = \exp\left(-\frac{1}{\dot{m}_{Na,t} \times c_{p,Na} \times R_{eq}}\right) \tag{5.29}$$

$R_{eq}$ is defined in Equation (5.30), and considers the heat transfer from the fluid to the external surface of the tube by convection and conduction. Equations (5.29) and (5.30) have been extracted from Reference [22].

$$R_{eq} = \frac{1}{h_{Na} \times \pi \times d_{in} \times L} + \frac{\ln\left(\frac{d_{ext}}{din}\right)}{2\pi \times k_t \times L} \tag{5.30}$$

Notice that the unknowns $\tilde{T}_t$ for the internal sodium flow and $E_t$ in the radiation circuit section, are in fact the same, due to the definition of the emissive power of the tube with the Stefan-Boltzmann law, which is expressed in Equation (5.31).

$$E_t = \sigma \tilde{T}_t^{\,4} \tag{5.31}$$

Equations (5.28) and (5.29) close the system once sodium properties, mass flow rate and the temperatures $T_1$ and $T_2$ are defined, which is done next.

### Mass flow rate

Along the following paragraphs, formulas to compute the mass flow rate are developed. However, the most important information of this paragraph is the explanation of the path followed by liquid sodium inside the receiver.

Sodium mass flow rate is a known parameter. In order to derive the expression to calculate it, it is necessary to take a look to Figure 5.6. In that sketch, it is shown how sodium exits the receiver with a temperature $T_{r,out}$ and, by transferring through the boiler $q_b$ to the water of the Rankine cycle, it losses temperature until reaching $T_{r,in}$ at the inlet of the receiver. All this can be expressed with Equation (5.32), which is used to compute directly the mass flow rate.

$$\dot{q}_b = \dot{m}_{Na} c_{p,Na} \left(T_{r,out} - T_{r,in}\right) \longrightarrow \dot{m}_{Na} = \frac{\dot{q}_b}{c_{p,Na} \left(T_{r,out} - T_{r,in}\right)} \tag{5.32}$$

It must be noticed, that by means of Equation (5.32) the total mass flow rate, the one flowing through the boiler, is calculated. However, this total $\dot{m}_{Na}$ is divided and follows different paths inside the receiver.

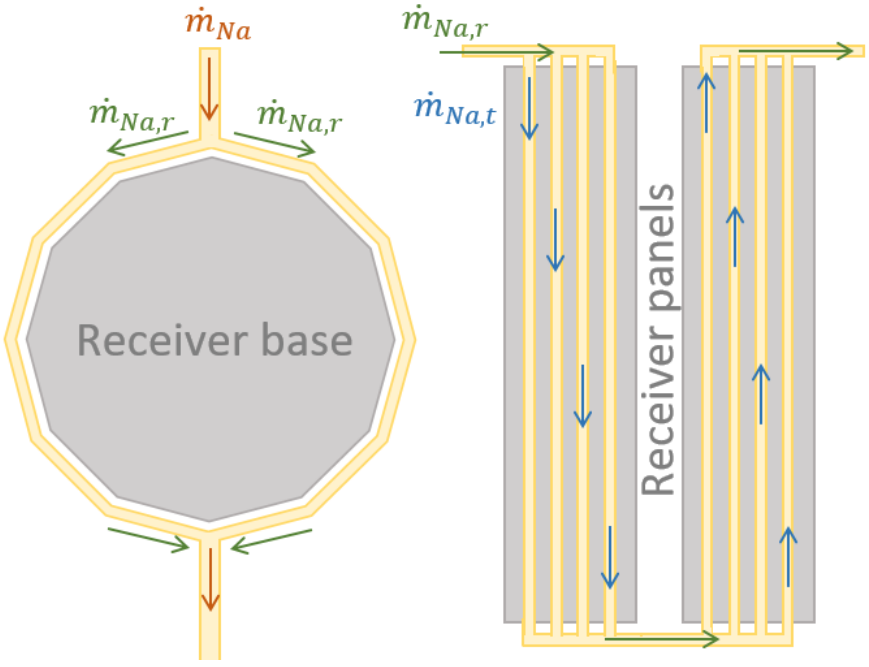


**Figure** 5.10: Path followed by liquid sodium inside the receiver

Figure 5.10 shows the path followed by sodium inside the receiver. As it is seen, liquid Na just passes through one half of the receiver, it does not follow the

complete revolution around the cylinder. For this reason, the total amount of sodium, represented with the red arrows in the left-hand side scheme of Figure 5.10, is split in two halves as soon as it enters into the receiver. Then, as observed in the panels depicted on the right side of Figure 5.10, the mass flow is divided among the tubes that each panel has, being reduced to $\dot{m}_{Na,t}$ (blue arrows) for each one.

Another fact that can be extracted from Figure 5.10 is that sodium moves from one panel to another changing the direction, i.e, through one panel Na moves downwards and in the next one it travels upwards.

Equations (5.33) and (5.34) show the expressions for computing $\dot{m}_{Na,r}$ and $\dot{m}_{Na,t}$ respectively.

$$\dot{m}_{Na,r} = \frac{\dot{m}_{Na}}{2} \tag{5.33}$$

$$\dot{m}_{Na,t} = \frac{\dot{m}_{Na,r}}{N_{tp}} = \rho_{Na} \times \pi \frac{d_{in}^2}{4} \times v_{Na} \tag{5.34}$$

Using Equation (5.34), it is possible to calculate the number of tubes per panel $N_{tp}$, which determines the dimensions of the receiver will be explained in Section 5.5.3. For this purpose, the value of sodium velocity, $v_{Na}$, is the only parameter that must be given for the design, since density $\rho_{Na}$ is computed with Equation 5.39, as is later explained, and the internal diameter is fixed as seen in Table 5.5. The only requirement that must be fulfilled by the velocity is that it must have a value between 1 and 5 $m/s$ so that not much losses are produced.

### Temperature distribution

To solve the receiver problem, it is needed to define $T_1$ and $T_2$. For doing so, it must be exactly understood what these temperatures represent and how the problem is faced.

As previously said, Equation (5.29) is only valid considering that the length L of the tube is small. Thus, for correctly using it, it is not possible to consider $T_1$ and $T_2$ as the temperatures $T_{r,in}$ and $T_{r,out}$ depicted in Figure 5.6, because that would imply that L would be the total length from the entrance of the receiver to its exit. A more correct possibility would be to choose the tube distance from one base of the cylindrical receiver to the other as L. However, it is more accurate to divide the tube distance between bases into different fragments, and analyse each of them separately, i. e., solve the problem once for each one of these pieces.

Therefore, what Figure 5.9 is showing is a small fragment of the complete path

followed by the working fluid through the receiver.

The temperature at the inlet and outlet of the receiver, which corresponds to $T_{r,in}$ and $T_{r,out}$ in Figure 5.6, are set and known. In the case of the inlet, the temperature selected is the melting temperature of sodium plus a safety margin of 40 °C. On the other hand, the outlet temperature is set as a design parameter, and some different values will be analysed to choose the best one in the final design.

Knowing $T_{r,in}$ and $T_{r,out}$, it is possible to know the temperature of sodium at any point in the receiver if a temperature profile is selected.

The chosen temperature profile could be anyone in principle. Then, depending on the defined distribution, the heliostat layout would be designed so that the radiation that the mirrors concentrate in the receiver would achieve the that designed temperature profile. However, there are some requirements that must be fulfilled by the heliostat field, and some temperature profiles would be better than others.

The goal is to build an heliostat field more or less uniform, as close to a circular shape as possible, enclosing the receiver at its center. To achieve this objective, the irradiance G computed for each fragment of the tube once the radiation circuit is solved must not differ a lot. In addition, it would be not physically possible to have two consecutive tube fractions with very different radiation. For these reasons, some temperature distributions will be tested and the one that best fits those requirements will be the selected one for solving the rest of the problem and design the receiver.

### Convective coefficient, $h_{Na}$

The convective coefficient depends on the properties and flow characteristics of liquid sodium inside the tubes.

For the computation of $h_{Na}$, three non-dimensional parameters are involved: Reynolds number, defined in Equation (5.35); Prandtl number, whose definition is written in Equation (5.36); and Nusselt number, which is defined in Equation (5.38). There is also a correlation among the three of them, written in Equation (5.37), which is only valid for a heated turbulent flow.

$$Re = \frac{\rho_{Na}\, v_{Na}\, d_{in}}{\mu_{Na}} \tag{5.35}$$

$$Pr = \frac{\mu_{Na}\, c_{p,Na}}{k_{Na}} \tag{5.36}$$

$$Nu = 0.023 \times Re^{0.8} Pr^{0.4} \tag{5.37}$$

$$Nu = \frac{h_{Na}\, d_{in}}{k_{Na}} \longrightarrow h_{Na} = \frac{Nu\, k_{Na}}{d_{in}} \tag{5.38}$$

The procedure to be followed is seen in the order of the four equations: Nusselt number is computed from the correlation (5.37) after solving the value of Re and Pr, and then, using Nu definition in Equation (5.38), the convection coefficient can be calculated.

### Sodium properties

As previously mentioned, molten sodium has been chosen for the receiver design due to its properties. It has a high boiling temperature and does not chemically react with the allow of which the tubes are made. Besides, the possible risk of explosion that molten sodium could have is eliminated in spite of the lack of oxygen in space and it can be used as well as the working fluid for the accumulation system.

The sodium properties that are required in order to solve the receiver problem are density, thermal conductivity, dynamic viscosity and specific heat capacity, all of them depending on temperature.

The purpose of this paragraph is to have the expressions of each of the properties enumerated above as a function of temperature, which must enter in the calculations expressed in Kelvin units. The following experimental correlations have been obtained from Reference [23].

$$\rho_{Na} = 219 + 275.32\left(1 - \frac{T}{2503.7}\right) + 511.58\left(1 - \frac{T}{2503.7}\right)^{0.5} \quad [kg/m^3] \tag{5.39}$$

$$k_{Na} = 124.67 - 0.11381T + 5.5226 \times 10^{-5} T^2 - 1.1842 \times 10^{-8} T^3 \quad [W/m \cdot K] \tag{5.40}$$

$$\ln \mu_{Na} = -6.4406 - 0.3958 \ln T + \frac{556.835}{T} \quad [Pa \cdot s] \tag{5.41}$$

As it is seen, Equation (5.39), (5.40) and (5.41) correspond to density, thermal conductivity and dynamic viscosity respectively. However, there is not a formula for computing the specific heat capacity of sodium as a function of temperature.

Therefore, in order to get it, a table given in Reference [23] with different values of $c_p$ for some temperatures is used, doing a linear interpolation to get a more precise number for the required temperature.

### 5.5.3 Receiver dimensions

One of the outputs to be extracted from the equations in Section 5.5.1 and 5.5.2 are the dimensions of the receiver. Figure 5.11 shows a sketch of the receiver with the main dimensions marked.

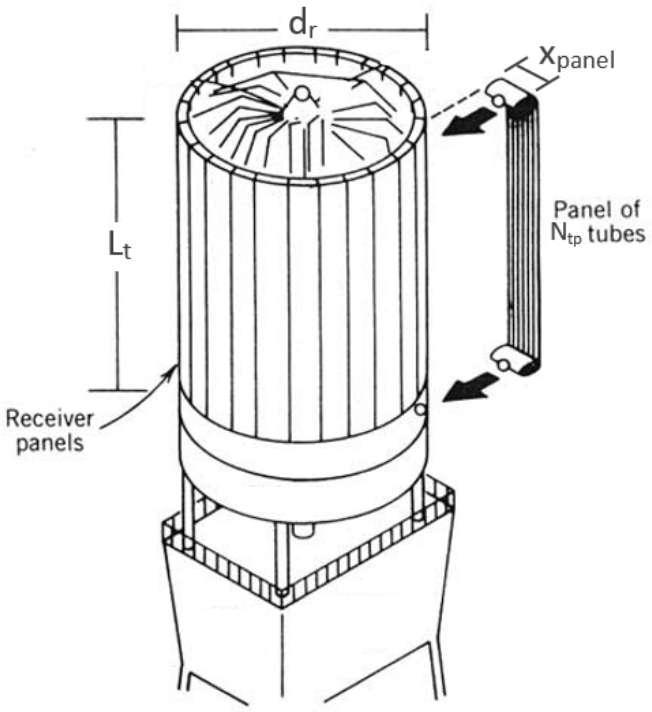


**Figure** 5.11: Receiver dimensions.
**Source:** Ref. [5] with modifications.

Once the number of tubes per panel, $N_{tp}$, is computed from Equation (5.34), the width of a single panel can be calculated using Equation (5.42).

$$x_{panel} = N_{tp} \times (d_{ext} + s) \tag{5.42}$$

Then, the total perimeter of the cylinder is obtained multiplying this width by the total number of panels that forms the receiver, as written in Equation (5.43). Finally, the diameter is computed with Equation(5.44).

$$P_r = N_{panels} \times x_{panel} \tag{5.43}$$

$$d_r = 2r_r = 2\frac{P_r}{2\pi} = \frac{P_r}{\pi} \tag{5.44}$$

One question that has not been considered until this point is how to select the number of panels of the receiver.

As said in Section 5.5.2 when talking about the temperature distribution, it is desired to have an irradiation G as constant as possible in all the receiver panels. The G distribution changes with the number of panels, as this number increases, sodium travels a greater distance inside the receiver. As the temperatures at the inlet and outlet of the receiver are set, the more distance travelled inside, the more progressively sodium can be heated and so the more constant would be the irradiation that must be provided by the heliostat field.

Therefore, in order to select the number of panels, a parametric analysis have been performed. Taking different values for $N_{panels}$ the complete problem is solved. Then, the lowest value of G that is computed for any tube fraction is subtracted to the highest one. In that way, it is possible to see which number of panels minimizes this difference, and thus, which is the number of panels to be chosen if a more or less constant G distribution is chased.

Finally, the receiver height must be computed. In this case, it is necessary to realize that the best design is a square receiver, that is, having $L_t$ as similar as the receiver diameter as possible. An heliostat reflects the solar radiation to a point in the receiver. However, the mirror has some dimensions, so the reflected ray is not going to reach the receiver in a single point. For this reason, if a very slender receiver is used, some concentrated irradiation would be wasted since it would not hit the panels.

Then, to compute the value of $L_t$, it has been assumed to be just the same as the receiver diameter, as expressed in Equation (5.45).

$$L_t = d_r \tag{5.45}$$

The last figure to compute in order to finish the receiver design is its performance, which is explained in the following section.

### 5.5.4 Receiver performance

Once the receiver problem is solved, it is possible to compute its performance with the simple expression written in Equation (5.46). As it is seen, the efficiency of the receiver is computed dividing the energy that the liquid sodium captures by the incident energy in the receiver coming from the heliostat field. The first one

corresponds to $q_b$, since no losses have been considered in the heat exchanged from sodium to water through the boiler. The term in the denominator, on the other hand, is computed by multiplying the irradiance times the area of the receiver panels.

$$\eta_r = \frac{\dot{q}_b}{G\, A_{panels}} \tag{5.46}$$

With this, all the information needed for solving the receiver problem is given. Then, the heliostat layout can be designed.

## 5.6 Heliostat field

After the receiver calculations, the heliostat field can be designed. In this section, the way in which heliostats are placed around the central receiver as well as the procedure to calculate the necessary number of them are explained. Besides, the expression to compute the mirror field performance is given at the end of the section.

It must be remembered at every point of the project that the thermosolar system that is being designed here is not built on a plain terrain on ground, it is a satellite orbiting the Earth. This means that the elements must be connected among them in some way and, it is maybe when dealing with the heliostat field, when this fact appears to be more important.

As there is not any ground nor gravity, there are a lot of new possibilities to connect all the elements. However, and as said before in this project, for simplicity the traditional configuration is the one to be implemented. The heliostats will be positioned following the layout that is explained in Section 5.6.1, all of them in the same plane. A beam structure would be the support for all the heliostats, having on its center a perpendicular beam acting as the tower, with the receiver on its end. At the base of the 'tower', the accumulation tanks and power system are located.

An advantage of having the thermosolar power plant orbiting around the Earth is that it is possible to control its orientation, which can be maintained always facing the Sun. For the calculations explained in this section, is is considered that the Sun remains always in the zenith with respect to the heliostat field. By doing this assumption, calculations are simplified and the amount of radiation reflected by heliostats only depends on their distance to the 'tower'.

### 5.6.1 Layout

When designing the heliostat field, it is important to take into account two effects: shadowing and blocking. The first one is produced when one of the heliostats is partially between the Sun and another heliostat. It is usual at low solar angles, so it might not be a problem for the present system design. Blocking, on the other hand, occurs when an heliostat interferes with the reflected radiation of another one [5].

In order to prevent these effects from happening, sophisticated computer programs as HELIOS or DELSOL2 have been implemented. However, a more basic method is used in this project, which is the radial stagger pattern shown in Figure 5.12.

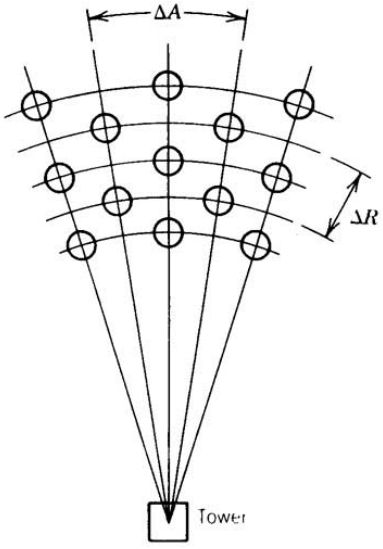


**Figure** 5.12: Radial stagger pattern.
**Source:** Ref. [5].

Heliostats are placed forming concentric rings around the tower. The parameters ΔR and ΔA shown in Figure 5.12 are calculated with Equations (5.47) and (5.48), respectively, which are optimized formulas developed by the University of Houston. In these equations, $HM$ accounts for the height of the mirrors and $WM$ to its width.

$$\Delta R = HM\left(1.44\cot\theta_L - 1.094 + 3.068\cdot\theta_L - 1.1256\cdot\theta_L^2\right)\ \ [m] \tag{5.47}$$

$$\Delta A = WM\left(1.749 + 0.6396\cdot\theta_L\right) + \frac{0.2873}{\theta_L - 0.04902}\ \ [m] \tag{5.48}$$

The angle $\theta_L$ is the altitude angle of the receiver from each of the heliostats, and is computed following Equation (5.49), in which $r$ is the normalized radius of the considered heliostat ring with the tower height.

$$\theta_L = \arctan\left(\frac{1}{r}\right) \tag{5.49}$$

As it is seen in Figure 5.12, with the radial stagger pattern, the heliostats are more separated from each other as the radius of the rings increases. In that way, the blocking effect is avoided. However, if many rings are needed to obtain the required reflected radiation in the receiver, there may be some point at which the mirrors are too far from each other and space is not used correctly. When this happens, the layout parameters are recalculated and a new pattern starts, producing a jump in the heliostat layout.

### 5.6.2 Number of heliostats

The way in which heliostats are placed around the receiver is given by the pattern just explained. What is left is to know how many mirrors must be used. To calculate this, it is necessary to equate the needed heat flux computed in the receiver design with the one reflected by the surrounding mirrors.

Regarding the receiver needed heat, it is simply computed by multiplying the irradiance $G$, which has $W/m^2$ units, obtained in the receiver design by the corresponding area. It is important to remember that a different G is obtained for each tube fraction, so that each value must be multiplied by the surface of the fraction, as expressed in Equation (5.50). In that equation, $d_{ext}$ is the external tube diameter, $L_t$ the receiver height and $N_{ft}$ the number of fractions per tube. Notice that just one half of the tube is considered, as the other one is not lit by sunlight.

$$q_G = G\left(\pi\frac{d_{ext}}{2} + s\right)\frac{L_t}{N_{ft}} \tag{5.50}$$

In order to compute the radiation reflected by each one of the heliostats to the receiver, the heliostat angle, $\theta_h$, must be defined. As seen in Figure 5.13, $\theta_h$ is the angle formed by the solar rays and the normal to the heliostat surface. It depends on the receiver height, $h_r$, and the radius of the corresponding heliostat ring, $r_h$. In addition, $\theta_h$ would change with the incidence angle of sun radiation, but for the present analysis, as previosly said, it is considered that the solar rays always come perpendicular to the plane in which mirrors are placed making the problem simpler. The expression to compute $\theta_h$ is given in Equation (5.51).

$$2\theta_h = \arctan\left(\frac{r_h}{h_r}\right) \tag{5.51}$$

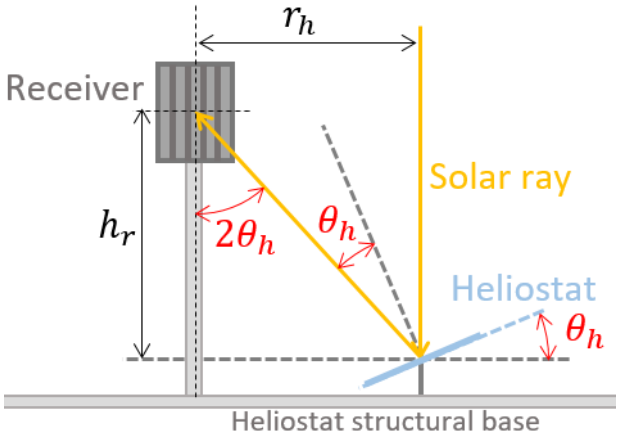


**Figure** 5.13: Heliostat angle definition.

The total radiation reflected to the receiver is the sum of the contributions of each mirror. Equation (5.52) shows how the total heat produced by the heliostats is computed, in which $G_s$ is the solar constant whose value is given in Table 5.2 and $A_h$ the heliostat area.

$$q_{rad} = \sum_j q_j = \sum_j G_s \, A_h \, \cos\theta_h^{(j)} \tag{5.52}$$

It is clear that $G_s$ does not change its value from one heliostat to another, because it is the solar constant. In addition, $A_h$ is also the same for all the mirrors since the same dimensions are maintained. Thus, the heat reflected by each heliostat is only dependent on the heliostat angle, which at the same time only changes with the heliostat radius $r_h$. This radius is the same for a given ring, so all the heliostats placed in the same row around the receiver provide the same amount of radiated heat to it.

Table 5.6 contains the heliostat dimensions as well as the height of the receiver with respect to the mirror plane. Heliostats used for the analysis have been considered square-shaped. In the thermosolar plant of Sevilla, Gemasolar, the heliostat dimensions are 10×10 meters [7], whereas for the studied case they have been reduced to 6×6 meters. The reason of this reduction with respect to the example of a ground-based thermosolar power plant is to make the construction of the satellite in space easier. The receiver heigh has been selected equal to the one used for the already mentioned Gemasolar power plant, although it could be optimized in a deeper study.

| **HM [m]** | **WM [m]** | **$h_r$ [m]** |
|---|---|---|
| 6 | 6 | 140 |

**Table** 5.6: Heliostat field dimensions.

To solve the heliostat field design, it is only needed to equate Equations (5.50) and (5.52), and place the necessary number of heliostats to get this equality following the radial stagger pattern previously explained.

### 5.6.3 Heliostat field performance

As for the case of the receiver, it is possible to compute the efficiency of the field of heliostats. This is calculated following Equation (5.53), which divides the total energy that reaches the receiver by the energy that would reach the mirrors if they were positioned totally perpendicular to the solar rays, as in the case of photovoltaic panels.

$$\eta_h = \frac{G\ A_{panels}}{G_s\ A_h} \tag{5.53}$$

With this equation the heliostat design is concluded, and the accumulation system can be sized.

## 5.7 Accumulation system

As it is already known, the thermosolar power satellite experiences an eclipse period during the orbit it describes around Earth. Throughout this time period, the solar rays do not reach the heliostats and they cannot reflect the radiation to heat liquid sodium and thus the power cycle cannot work.

If an uninterrupted electric production is required, there must be included in the design an accumulation system. Going back to Figure 2.5, it can be appreciated the way in which the accumulation system is designed. It consists on two separated tanks, one storing cold liquid sodium and the other containing this fluid at the temperature that it exits the receiver. In that way, when there is no solar radiation to heat up liquid Na, the stored hot one is used to power the Rankine cycle.

The design of the storage system to be developed in this section consists just on a rough approximation to have a global idea of what would be the dimensions required to have a continuous production of electric power.

The relation between the lit time period and the one in which the satellite remains behind the Earth shadow is given in Equation (5.54). This formula expresses that the energy received by the receiver when there is solar radiation present must be equal to the energy that the system needs to be able to work during the complete orbit.

$$W_{receiver} \cdot T_l = \frac{W_{electric}}{\eta_{total}} \cdot T_o \tag{5.54}$$

$W_{receiver}$ accounts for the power that the receiver must collect during the lit period $T_l$; $W_{electric}$ is the required electric power for which the system is designed; $T_o$, the period of the complete orbit; and $\eta_{total}$ the efficiency that, as seen in Equation (5.55), takes into account the mechanical and thermal inefficiencies, $\eta_m$ and $\eta_{th}$, respectively.

$$\eta_{total} = \eta_{th} \cdot \eta_m \tag{5.55}$$

From Equation (5.54), $W_{receiver}$ is computed, and with it, the energy to be stored in the hot tank can be calculated using Equation (5.56).

$$E_{tank} = \left( W_{receiver} - \frac{W_{electric}}{\eta_{total}} \right) \times T_l \tag{5.56}$$

The mass of liquid sodium needed to store $E_{tank}$ is obtained following Equation (5.57), knowing the difference in temperature through the receiver and the specific heat capacity, computed with the temperature as explained in the sodium properties paragraph in Section 5.5.2. Also with the procedure that is written in that paragraph, the density of sodium at the mean temperature through the receiver can be obtained, and the volume of the tank is readily calculated using Equation (5.58). Notice that a safety margin $SM$ is used in the tank volume calculation.

$$m_{Na} = \frac{E_{tank}}{c_p \left( T_{r,out} - T_{r,in} \right)} \tag{5.57}$$

$$V_{tank} = SM \cdot \frac{m_{Na}}{\rho_{Na}} \tag{5.58}$$

With the tank volume known, what is left is to decide which will be its shape and define its dimensions. Following the real case of Gemasolar, cylindrical tanks are chosen, although any other shape (such as a spherical container) is possible. The volume of a cylinder as a function of its radius $r_{tank}$ and height $h_{tank}$ is expressed in Equation (5.59), and its complete surface in Equation (5.60).

$$V_{tank} = \pi r_{tank}^2 \cdot h_{tank} \tag{5.59}$$

$$S_{tank} = 2\pi r_{tank}^2 + 2\pi r_{tank} \cdot h_{tank} \tag{5.60}$$

With the volume and surface equations, the height of the tank can be eliminated from the problem, and the surface as a function of $r_{tank}$ only can be extracted, as Equation (5.61) shows. Then, the derivative of the surface is taken and equated to zero, in order to minimize it, and finally the radius of the tank is get, as seen in Equation (5.62).

$$S_{tank} = 2\pi r_{tank}^2 + 2 \times \frac{V_{tank}}{r_{tank}} \tag{5.61}$$

$$\frac{\partial S_{tank}}{\partial r_{tank}} = 0 \quad \longrightarrow \quad r_{tank} = \sqrt[3]{\frac{V_{tank}}{2\pi}} \tag{5.62}$$

In order to compute the height of the tank, it is only needed to solve it from Equation (5.59) once the radius is known.

Notice that this procedure is valid for both the cold and the hot tank, and that the only difference is the density to be used in Equation (5.58), which makes a small difference in the dimensions of each one.

# Chapter 6

# Results

After all the methodology has been explained in detail, the design results can be obtained. This chapter contains the outcome of all what has been explained along this project.

In addition to the numerical results, an analysis is done in order to select some parameters that are not fixed in the problem, as it is the number of panels of the receiver, the temperature profile of liquid sodium and the outlet temperature of the receiver.

## 6.1 Orbit parameters

Using the formulas stated in Section 5.3, the eclipse period and surrounding temperature of the ISS orbit are computed.

### 6.1.1 Eclipse period

For computing the eclipse period, Equations (5.1)-(5.3) are used. All the necessary data is given in Table 5.1, except the solar angle $\beta$, which is represented graphically in Figure 5.3.

The obtained results for the orbit and eclipse period are summarized in Table 6.1. In addition, the lit period $T_l$ and the eclipse fraction are given in the third and fourth column respectively. With the eclipse fraction, it is possible to better see the period of time that the satellite remains at shadow compared to the total orbit.

| $\mathbf{T}_o$ [min] | $\mathbf{T}_e$ [min] | $\mathbf{T}_l$ [min] | $\mathbf{T}_e/\mathbf{T}_o$ [-] |
|---|---|---|---|
| 92.02 | 34.80 | 57.22 | 0.3782 |

**Table** 6.1: Orbit and Eclipse period results.

As it is seen, more than a third of the total time during which the thermosolar power satellite is performing a complete revolution around the Earth, happens without solar light. This means that, during that time, solar rays do not reach the heliostat field and no power can be produced unless an accumulation system is installed.

The design of the accumulation system is developed in Section 6.5.

### 6.1.2 Effective surrounding temperature

Following the procedure explained in Section 5.3.2 and using Equation (5.7), it is possible to get the temperature at the receiver surroundings, which is expressed in Table 6.2.

| $T_s$ [K] |
|---|
| 342.59 |

**Table** 6.2: Temperature at the surroundings of the receiver.

The obtained result for the effective surrounding temperature corresponds to 69.43ºC, which is almost 70ºC. This value seems to be reasonable.

In Reference [24], a range of values for the surrounding temperature for the ISS orbit is given. This range goes from -120ºC when the International Space Station is moving along the Earth shadow, to a maximum temperature of 120ºC when sunlight is reaching it.

The temperature of interest for the following calculations is the one that the receiver feels when it is exposed to sunlight, so a maximum of 120ºC is expected. However, a significant reduction in this number is observed, and it is due to the fact that the solar radiation does not hit the receiver panels, it goes parallel to them so a small fraction of it contributes to the effective surrounding temperature, as was considered in Equation (5.7).

## 6.2 Power cycle

From the Rankine cycle it is interesting to obtain the heat in and out so that the required design power is obtained. The heat entering through the boiler, $\dot{q}_b$, is needed for dimensioning the receiver and heliostat field. On the other hand, the heat going out of the system through the condenser is used for the design of the heat pipes. Table 6.3 contains these two results, that are obtained following the methodology explained in Section 5.4. In addition, the value of the thermal efficiency of the cycle is given.

| $\dot{q}_b$ [MW] | $\dot{q}_c$ [MW] | $\eta_{th}$ [-] |
|---|---|---|
| 3.73 | 2.46 | 0.34 |

**Table** 6.3: Results obtained in the Rankine cycle.

## 6.3 Receiver dimensions

In this section, the dimensions of the receiver are finally selected. The first step is to choose the temperature distribution that gives the best results considering the requirements to be fulfilled by the heliostat field layout. Once the temperature profile is selected, the problem will be solved for different temperatures at the outlet of the receiver in order to see how the design changes and choose the best one.

### 6.3.1 Temperature distribution

The first step in the receiver design deals with the selection of the temperature profile of the molten sodium that travels through it, which will be created thanks to the heliostat field distribution. For each one of the three temperature profiles that will be analysed in this project, the number of panels and the dimensions of the receiver will change, and a correct choice must be done taking into consideration the following statements:

- The irradiance G cannot reach a value greater than 1 $MW/m^2$ at any point of the receiver. This is the typical limit used in order to avoid high temperature gradients in the tubes that can produce thermal fatigue or even melt its walls.

- It is not physically possible to have a significant jump in the G distribution for consecutive tube fractions.

- The difference between the greatest and lowest value for G in the whole

receiver must be as small as possible in order to have a more or less uniform heliostat field.

- The less number of panels required for the receiver, the better, because less mass is put into orbit and so, cheaper is the construction of the space-based solar power system. This also applies for the heliostat number.

For the selection of the temperature distribution, a fixed value for the temperature of the molten sodium at the outlet of the receiver is chosen. The selected $T_{r,out}$ is written in Table 6.4. This value has been selected because it is considered as a conservative typical value that exceeds 100ºC the Rankine cycle temperature $T_3$, assuring that the heat exchanger area between water and molten sodium is not very large. Later, along Section 6.3.2, the effects of changing the value of $T_{r,out}$ are studied.

| $\mathbf{T}_{r,out}$ [ºC] |
|---|
| 700 |

**Table** 6.4: Fixed $T_{r,out}$ for the selection of temperature profile.

Within this section, the receiver problem that was explained in Section 5.5 is solved for three different temperature profiles: linear, logarithmic and parabolic. For each one of them, the optimum number of panels is selected taking into account the considerations enumerated above.

Firstly, the most simple distribution was proven, which is the linear one. As it is possible to see later in Figure 6.3 (a), the irradiance map obtained with the linear profile shows that the G must be increased as sodium is flowing through the tubes until the last panel.

As it has been mentioned, one of the objectives is to create an heliostat field as regular as possible, which is translated in an irradiance distribution as constant as possible for all the receiver panels. For that purpose, it was necessary to find a temperature profile that rises the irradiance in the first panels. Two functions were developed for doing so: a logarithmic and a quadratic parabola.

Figure 6.1 shows the three temperature profiles. As it is seen, the logarithmic function produces a stronger temperature rise in the first panels if compared to the parabola, which is softer.

In the following paragraphs, these three temperature profiles are tested. For each one, the receiver problem is solved for a range of possible number of panels. For each $N_{panels}$, the maximum and minimum value of G are plotted in order to select the optimum number of panels that minimizes the difference between $G_{max}$ and $G_{min}$ and does not overpass the irradiance limit.

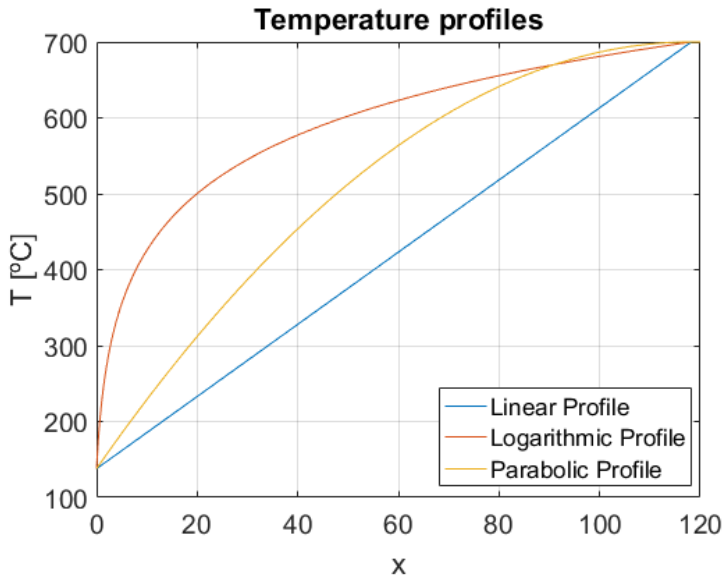


**Figure** 6.1: Temperature profiles of molten sodium inside the receiver tubes.

Then, with the chosen number of panels, the G map is plotted and a comparison is done between the three temperature profiles, to choose the best one for the design.

### Maximum and minimum G for different number of panels

Figure 6.2 shows the maximum and minimum values of G reached in the receiver for different number of panels and for each one of the temperature profiles.

The number of panels range that is analysed in the graphs goes from 20 to 50 panels. Notice that this number of panels corresponds, really, to half of the receiver, which is the path followed by liquid sodium. When computing the receiver dimensions, the total number of panels needs to be taken into account.

The green line in the three plots represents the limit of 1 $MW/m^2$ previously explained, which cannot be overpassed. As it is seen in Figure 6.2 (b), for the logarithmic temperature profile, the maximum G value is always far above the limit in the range of number of panels considered. This fact eliminates the logarithmic profile option from the selection. Regarding the linear and parabolic distributions, and considering the green limit, it is seen that the minimum possible number of panels is 34 and 42, respectively.

Another characteristic that must be analysed is the difference between the maximum and minimum irradiance. The lower this difference, the more uniform the heliostat field, so the better option for the design. For the linear profile in Figure 6.2 (a), it seems that the difference between both curves increases slightly with the number of panels. However, this rise is not very significant, specially when comparing it with the parabolic case in Figure 6.2 (c), whose minimum difference,

reached with 50 panels, is still higher than the greatest one observed for the linear plot.

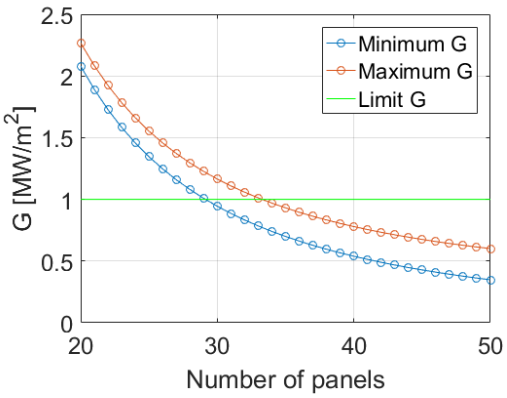


(a) Linear distribution.

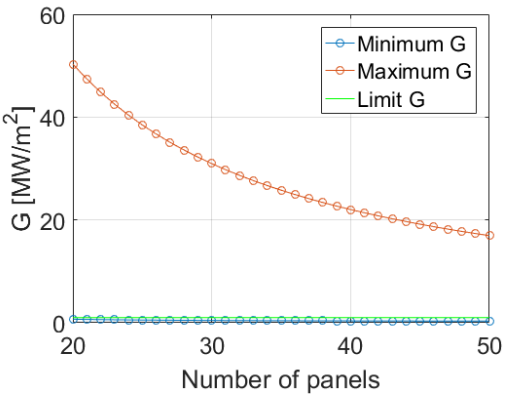


(b) Logarithmic distribution.

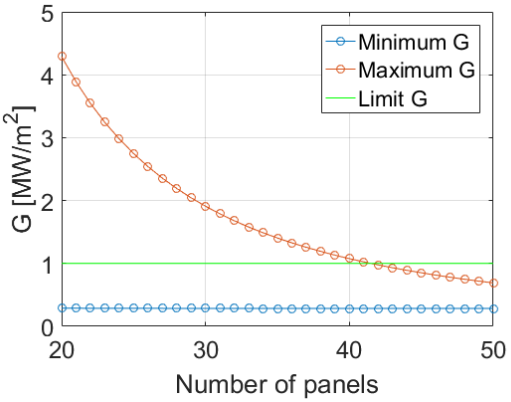


(c) Parabolic distribution.

**Figure** 6.2: Maximum and minimum G evolution as a function of the number of panels.

After this analysis, it seems clear that the linear temperature profile is more advantageous than the parabolic one, and, needless to say, much better than the logarithmic, which does not fulfil any of the requirements.

However, it is still necessary to see the irradiance map and detect whether or not there are big jumps in the G reached in adjacent tube fractions. If this is the case, a linear temperature profile would not be physically possible.

### Irradiance map for selected number of panels

Considering the minimum number of panels obtained for each temperature profile by looking at Figure 6.2, the irradiance maps are represented so that it is possible to see how G is distributed in the receiver panels and whether this distribution is physically possible or not.

Table 6.5 contains the selected points of Figure 6.2 that are used for the G map representations of Figure 6.3.

| | **Linear** | **Logarithmic** | **Parabolic** |
|---|---|---|---|
| **Number of panels** | 34 | 50 | 42 |
| **Maximum G** $[MW/m^2]$ | 0.97 | 16.94 | 0.98 |
| **Minimum G** $[MW/m^2]$ | 0.74 | 0.32 | 0.28 |

**Table** 6.5: Selected points to get minimum number of panels for each temperature distribution.

As already mentioned, the selection criteria has been the minimum number of panels to have an irradiance lower than 1 $MW/m^2$ at every point of the receiver. For the case of the logarithmic distribution, this is not possible in the studied range of number of panels, so the best case, which corresponds to the point at 50 panels, is chosen for the G map, just to see its shape.

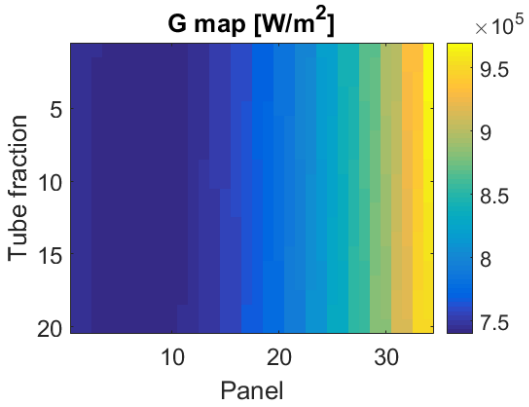


(a) Linear distribution.

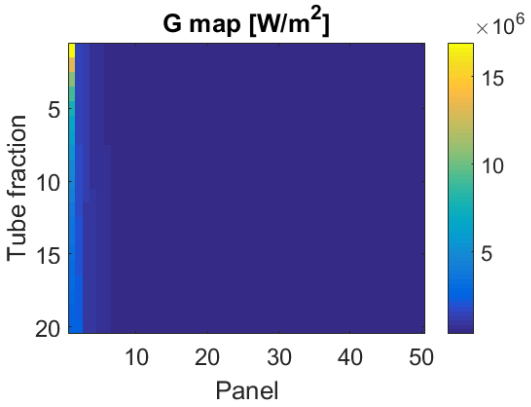


(b) Logarithmic distribution.

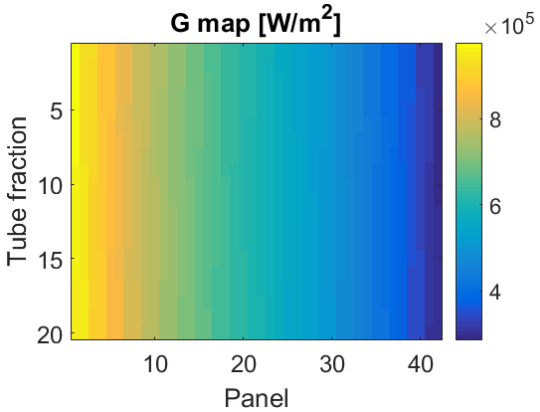


(c) Parabolic distribution.

**Figure** 6.3: Irradiance map for the minimum possible number of panels for each temperature profile.

By looking at Figure 6.3 (a) and (c), it is seen how both the linear and parabolic distribution follow a progressive change in G. For the case of the linear profile, the irradiance increases in the panels as the working fluid is passing through them. In contrast to this behaviour, the G when a parabolic profile is selected decreases as liquid sodium is heated up. This is due to the fact that in the parabolic profile the temperature increases more at the beginning than at the end of the receiver, as seen in Figure 6.1.

Regarding the logarithmic profile, irradiance reaches a very high peak in the first fragment of the tube in the first panel, and then remains almost constant. This is not physically possible for two reasons: firstly, there is a huge difference between the value of G in adjacent tubes and even in consecutive fractions of the same tube; secondly, the values of G are above the limit of 1 $MW/m^2$.

Coming back to the linear and parabolic profiles, it seems that the progressive change in G occurs more uniformly in the parabolic case, but the difference between maximum and minimum is much lower for the linear profile. As the number of panels are also less for the linear, it seems that the profile to choose is this one. However, both profiles are going to be analysed in the heliostat field layout, in order to take also into account the needed number of heliostats and have a global comparison of both options.

### 6.3.2 Analysis with different values for $T_{r,out}$

Now that the temperature profile has been analysed, the effect of the temperature at the outlet of the receiver is studied. For doing so, three different temperatures are going to be defined and both the graph for the maximum and minimum G depending on the number of panels and the irradiance map are compared. In addition, the study is done for the linear and parabolic temperature profiles.

The value of the temperature at the outlet of the receiver for the three different cases to by studied in this section is written in Table 6.6. Notice that the Case 2 corresponds to the results already obtained in Section 6.3.1.

| | **Case 1** | **Case 2** | **Case 3** |
|---|---|---|---|
| $\mathbf{T}_{r,out}$ **[ºC]** | 500 | 700 | 900 |

**Table** 6.6: Values of the temperature at the exit of the receiver to be analysed.

One could think that Case 1 does not make any sense, since the temperature selected for water inside the Rankine cycle at the boiler $T_3$, whose value is 600ºC, is greater than the temperature of sodium at the exit of the receiver. However, the analysis performed in this section only considers the receiver, isolating it from the rest of the components just to see the effect that the change of $T_{r,out}$ would produce on its size. Of course, if Case 1 was selected for the receiver, the Rankine

cycle might be redesigned in order to have a lower $T_3$.

Once this fact has been clarified and before seen the results, it is important to have in mind all the figures that are affected by a change in $T_{r,out}$.

It is needless to say that, by changing the value of the receiver outlet temperature, the values of the temperatures at each point of the receiver change and its corresponding sodium properties, as well as the global solution of the receiver system of equations and the irradiacion values as a consequence of it, as it is seen in the following graphs and colour maps.

However, another important effect can be anticipated. Going back to Equation 5.32 it is seen how the outlet temperature has an important effect in the sodium mass flow. The heat exchanged in the boiler from Na to water remains constant, since the Rankine cycle parameters are fixed for the study performed in this project. For this reason, if the outlet temperature increases, the mass flow is reduced. This reduction in the mass flow produces, at the same time, a reduction in the number of tubes per panel, as seen in Equation (5.34), which will produce a decrease in the dimensions of the receiver.

In the tables shown below, the number of tubes per panel for each $T_{r,out}$ is included. Notice that this number is not affected by the temperature profile selected, it is just a function of the temperature at the outlet.

### Linear temperature profile

Using the linear temperature profile, it is seen that, as $T_{r,out}$ increases, so does the minimum number of panels that allows to be under the limit at every point of the receiver.

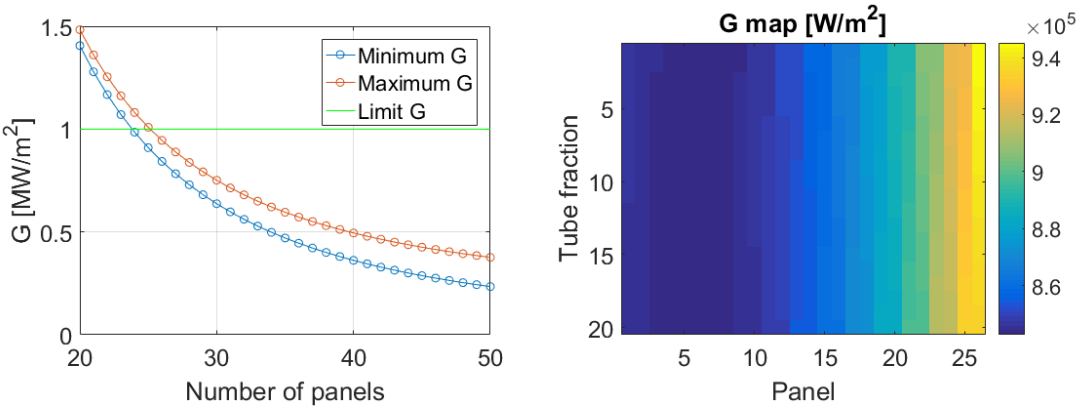


(a) G max and min distribution.

(b) G map for minimum number of panels.

**Figure** 6.4: Results for Case 1 with the linear temperature profile.

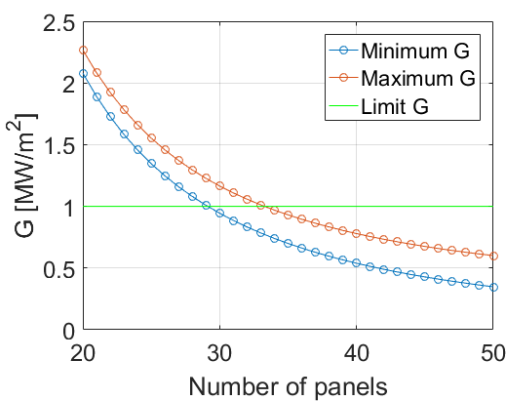


(a) G max and min distribution.

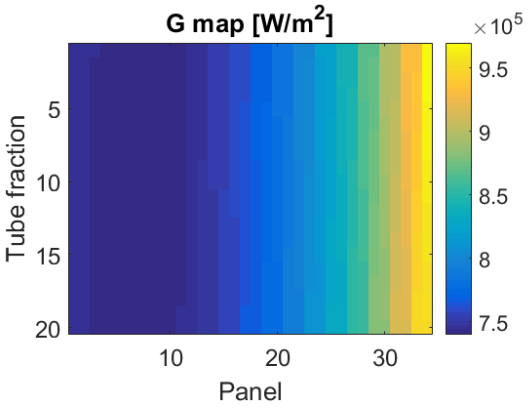


(b) G map for minimum number of panels.

**Figure** 6.5: Results for Case 2 with the linear temperature profile.

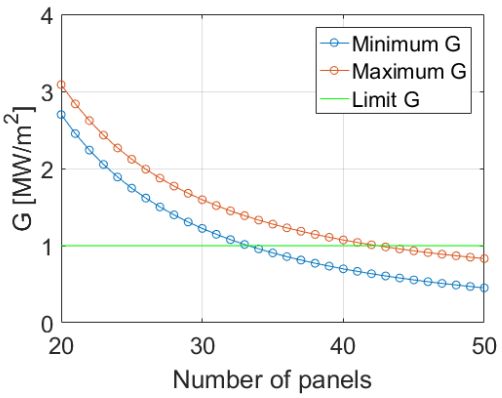


(a) G max and min distribution.

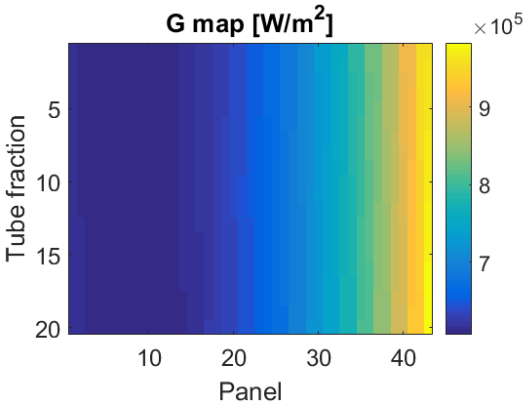


(b) G map for minimum number of panels.

**Figure** 6.6: Results for Case 3 with the linear temperature profile.

The G map follows the same distribution in the three cases, but looking at the colour scale in the right, it is seen that as the temperature is increased, the range of values that the irradiance reaches is wider.

| **LINEAR PROFILE** | **Case 1** | **Case 2** | **Case 3** |
|---|---|---|---|
| **Number of tubes per panel** | 9 | 6 | 4 |
| **Number of panels** | 26 | 34 | 43 |
| **Maximum G** $[MW/m^2]$ | 0.94 | 0.97 | 0.98 |
| **Minimum G** $[MW/m^2]$ | 0.84 | 0.74 | 0.61 |

**Table** 6.7: Selected points to get minimum number of panels for each $T_{out}$ case with linear temperature profile.

These two facts are better seen in Table 6.7, in which the minimum number of panels for each case is written, as well as the maximum and minimum values of G obtained with it.

### Parabolic temperature profile

With the parabolic profile, similarly to the linear one, the minimum possible number of panels increases with temperature.

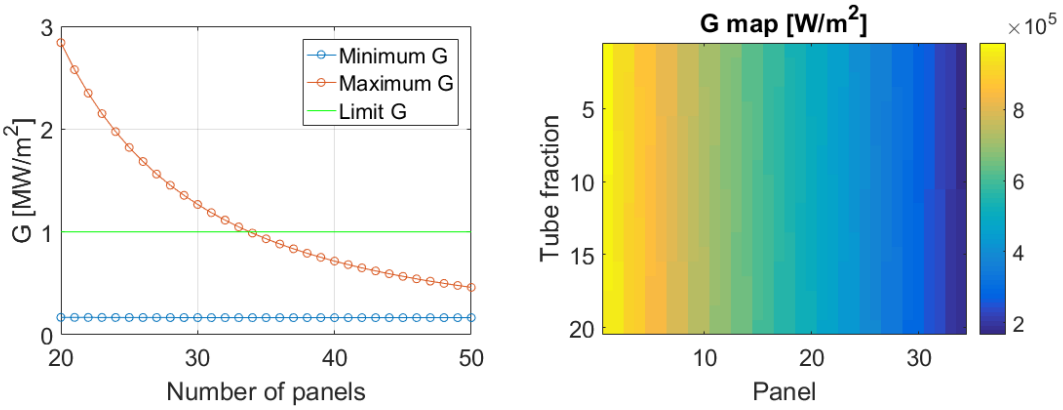


(a) G max and min distribution. (b) G map for minimum number of panels.

**Figure** 6.7: Results for Case 1 with the parabolic temperature profile.

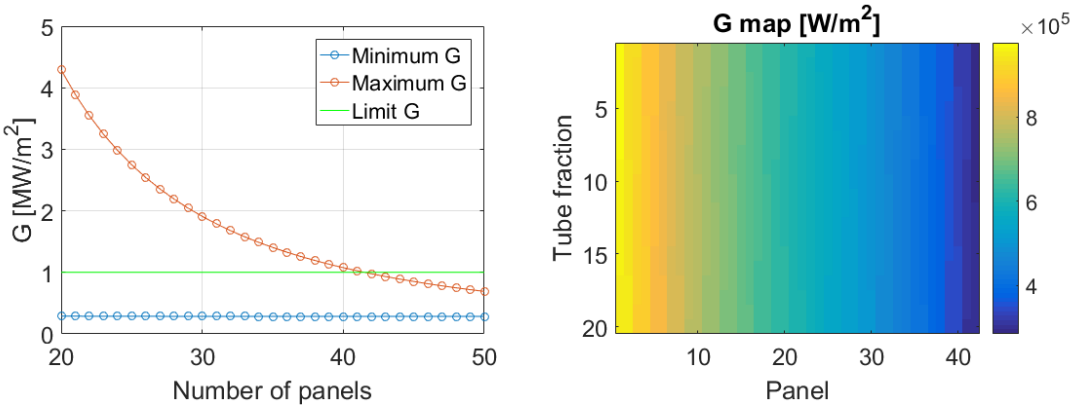


(a) G max and min distribution. (b) G map for minimum number of panels.

**Figure** 6.8: Results for Case 2 with the parabolic temperature profile.

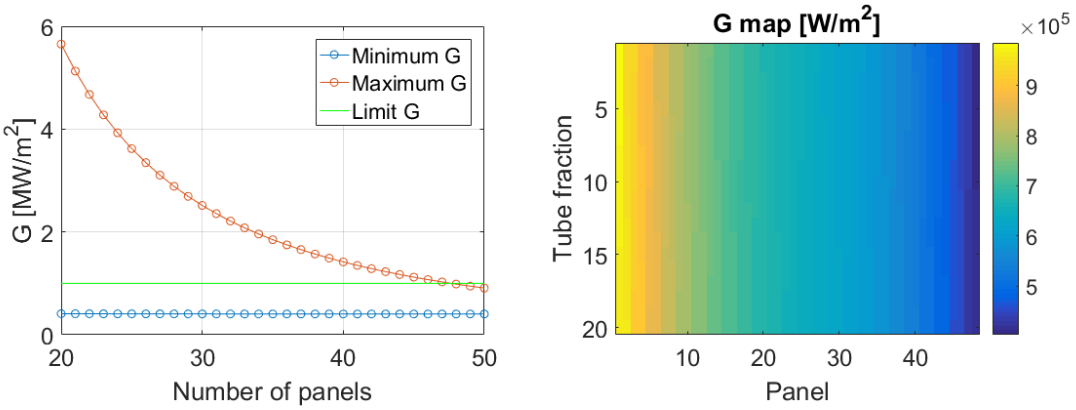


(a) G max and min distribution.

(b) G map for minimum number of panels.

**Figure** 6.9: Results for Case 3 with the parabolic temperature profile.

The irradiance map also has the same appearance, but in this case it seems to reduce the difference between minimum and maximum values. However, this conclusion is not completely true. As $T_{r,out}$ increases, the point of minimum possible number of panels is moved to the right in the graph. This effect makes by itself a reduction in the difference between extreme values of G. If an equal number of panels is compared for the three cases, it turns out that as temperature increases, the separation between the red and blue curves rises too.

| **PARABOLIC PROFILE** | **Case 1** | **Case 2** | **Case 3** |
|---|---|---|---|
| **Number of tubes per panel** | 9 | 6 | 4 |
| **Number of panels** | 34 | 42 | 48 |
| **Maximum G** $[MW/m^2]$ | 0.99 | 0.98 | 0.98 |
| **Minimum G** $[MW/m^2]$ | 0.17 | 0.28 | 0.40 |

**Table** 6.8: Selected points to get minimum number of panels for each $T_{out}$ case with parabolic temperature profile.

### 6.3.3 Receiver Geometry

Following the methodology explained in Section 5.5.3, it is possible to get the receiver dimensions. Remember that the computations have been done forcing the diameter of the receiver to be the same as its height, so that the lateral view of the cylinder is a square. In Tables 6.9 and 6.10, the receiver diameter is finally computed, and the number of panels and tubes per panel are also displayed.

From this results, it can be concluded that the number of tubes per panel has a greater effect on the receiver diameter than the number of panels. It is seen that,

as $T_{r,out}$ increases, there are less tubes per panel and a reduction in the dimensions is produced, even though the number of panels increases. Indeed, the important figure for selecting the better choice is the product between both numbers, which accounts for the total number of tubes in the receiver.

| **LINEAR PROFILE** | **Case 1** | **Case 2** | **Case 3** |
|---|---|---|---|
| **Number of tubes per panel** | 9 | 6 | 4 |
| **Number of panels** | 26 | 34 | 43 |
| **Receiver diameter [m]** | 4.27 | 3.73 | 3.14 |

**Table** 6.9: Receiver geometry results for the linear temperature profile.

| **PARABOLIC PROFILE** | **Case 1** | **Case 2** | **Case 3** |
|---|---|---|---|
| **Number of tubes per panel** | 9 | 6 | 4 |
| **Number of panels** | 34 | 42 | 48 |
| **Receiver diameter [m]** | 5.59 | 4.60 | 3.51 |

**Table** 6.10: Receiver geometry results for the parabolic temperature profile.

Taking into account the complete receiver analysis, it seems that the better option is the linear temperature profile with a $T_{r,out}$ of 900 °C.

One could think that, if this temperature is increased above 900 °C, the dimensions could be reduced even more. However, the temperature used for Case 3 is already the maximum temperature that can be safely achieved by sodium without causing any damage in the receiver materials.

### 6.3.4 Receiver performance

Following the expression written in Equation (5.46), it is possible to get the efficiency of the receiver. The obtained value is presented in Table 6.11. Notice that temperature of Case 3 has been used for the calculations.

| $\eta_r$ [-] |
|---|
| 0.22 |

**Table** 6.11: Receiver performance considering Case 3.

The obtained value seems to be very small. In fact, it is smaller than the one

given for the photovoltaic cells in Chapter 2. This may be produced because the calculations done in this work can be further improved and optimized as it is later explained in Chapter 7. However, although the efficiency of the thermosolar power satellite may be lower than the one of the photovoltaic cells, the conversion system devoted in this project would be the option to choose, because the efficiency of PV panels decreases when large amounts of electricity are produced. In addition, this amount of energy cannot be stored in any electric battery that exists nowadays. Considering that more than a third of the total time the satellite takes to perform a complete orbit it remains in the Earth shadow, the accumulation of energy is an important fact and so the thermosolar technology would be better since by storing thermal energy is able to accumulate the large amount of power needed.

## 6.4 Heliostat field

When solving the receiver problem it has been demonstrated that, for any $T_{r,out}$, the results obtained defining the temperature profile as linear are better than the parabolic distribution ones. For this reason, the calculations performed for the heliostat field design only consider the linear temperature profile inside the receiver, and are done for the three different cases of $T_{r,out}$ to compare them.

In the present section, Equation (5.50) is solved using the G distribution previously calculated for each outlet temperature case. Then, heliostat coordinates are computed with the radial stagger pattern explained in Section 5.6.1 until the value for $q_{rad}$ obtained with Equation (5.52) is as close as possible to the value of $q_G$.

As it has been observed along Section 6.3, the value of G is not constant for all the receiver. For this reason, the heliostat problem is solved by dividing the receiver in eight sections, which means four sections in the computations since just a half of the cylinder is solved, being the other one symmetrical to it. In that way, the heliostat field is also divided in four sections, each one containing the needed mirrors to produce the heat given by the G in each receiver section.

Figures 6.10, 6.11 and 6.12 shows the G map for the three temperature cases, together with the heliostat field calculated for each one. The numerical results of $q_G$, $q_{rad}$ and the number of heliostats for the three cases are summarized in Table 6.12.

| | **Case 1** | **Case 2** | **Case 3** |
|---|---|---|---|
| **$q_G$ [MW]** | 76.35 | 53.21 | 33.18 |
| **$q_{rad}$ [MW]** | 76.16 | 53.04 | 32.94 |
| **Number of heliostats** | 1702 | 1166 | 712 |

**Table** 6.12: Heliostat field results for the three $T_{r,out}$ cases.

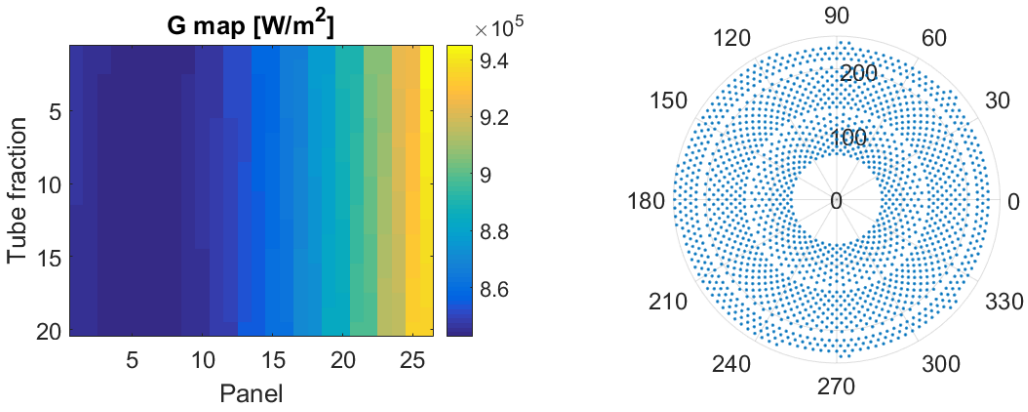


(a) G map. (b) Heliostat field.

**Figure** 6.10: Heliostat field obtained for Case 1.

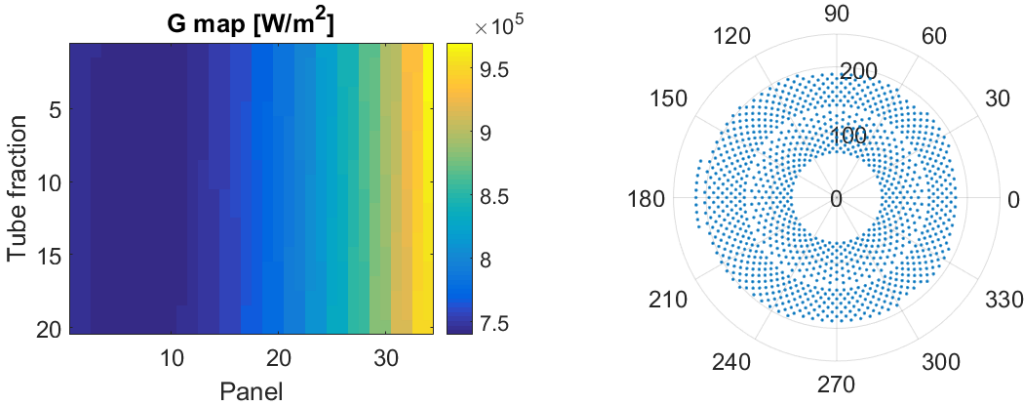


(a) G map. (b) Heliostat field.

**Figure** 6.11: Heliostat field obtained for Case 2.

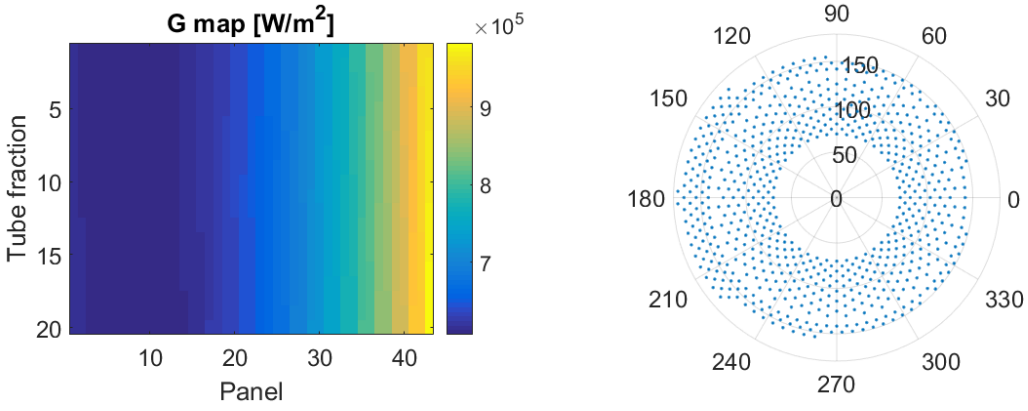


(a) G map. (b) Heliostat field.

**Figure** 6.12: Heliostat field obtained for Case 3.

By observing the obtained results, it can be seen how by increasing the outlet receiver temperature, the necessary heat decreases and thus, the number of heliostats. This behaviour may seem contradictory at a first look, but it can be easily explained.

Remember that the selection criteria for the number of panels performed in Section 6.3 was to choose the minimum possible number attending to the irradiance limit of 1 $MW/m^2$. This implies that, for the three cases, the maximum value reached by G in the receiver is almost the same, a bit smaller than the limit. Then, different minimum values are seen in each case, as written in Table 6.7, being higher and thus producing a more constant distribution for 500 ºC than for 900 ºC. Taking into account this fact, it can be said that, if the dimensions of the receiver were the same, more heat would be needed for Case 1 than for Case 3, as the mean of G through all the receiver is higher.

However, dimensions of the receiver are not the same for all the temperatures, as was seen in Table 6.9. The higher the temperature at the exit of the receiver, the lower the diameter, because lower is the total number of tubes. Therefore, the surface of the receiver reaches its smallest value with the higher temperature, and when multiplying by the irradiance, the obtained heat is lower than the one got for the other two cases, which is the result observed in Table 6.12.

Two additional features of the obtained results may be commented. The first one is that, as already mentioned in previous sections, the heliostat field is more uniform and more circular-shaped for low values of the receiver exit temperature. This happens because the G map is also more constant at these cases.

The second deals with the fact that $q_G$ and $q_{rad}$ are not exactly the same. As the heliostat size is predetermined, the exact heat obtained from the receiver problem can not be reached. The values of $q_{rad}$ given by the heliostats placed in the field is slightly lower than the ones of $q_G$, but adding just one mirror more, this value would be higher. The point is that it does not matter whether this value is slightly higher or slightly lower, the difference is just one heliostat, which does not change anything for comparison purposes.

With the results obtained in this section, it is finally checked that the best configuration for the receiver is the linear profile with an outlet temperature of 900ºC, because not only a smaller receiver is needed, but also less number of heliostats, which is translated in a reduction in material and mission costs to put all the elements in orbit.

To finish with this section, is is possible to compute the heliostat performance from Equation (5.53). The result is given in Table 6.13, which is almost a 50%.

This result is highly dependant on the inclination of heliostats in order to direct the solar rays that they reflect towards the receiver. It could be improved by a different location of the heliostats, following a more efficient distribution computed

by more sophisticated methods that the one used in the present work.

| $\eta_h$ [-] |
|---|
| 0.47 |

**Table** 6.13: Heliostat field performance.

## 6.5 Accumulation system

Following the procedure explained in Section 5.7, the dimensions of both the cold and hot cylindrical tanks for the accumulation system can be computed. The obtained results, that has been compute for a $T_{r,out}$ of 900 ºC, are summarized in Table 6.14.

| | **Hot tank** | **Cold tank** |
|---|---|---|
| $\mathbf{m}_{Na}$ [t] | 8.35 | 8.35 |
| $\mathbf{V}_{tank}$ [$\mathbf{m}^3$] | 11.84 | 14.70 |
| $\mathbf{r}_{tank}$ [m] | 1.23 | 1.33 |
| $\mathbf{h}_{tank}$ [m] | 2.47 | 2.65 |

**Table** 6.14: Dimensions of the accumulation tanks.

As it is observed, dimensions of the cold tank are slightly greater than dimensions of the tank storing the hot sodium. This result was expected due to the difference in density between cold and hot liquid sodium. The mass of sodium is the same for both tanks, and was calculated following Equation (5.57). However, as temperature of Na increases, so does its density, and the higher the density, the lower the volume it occupies.

# Chapter 7

# Conclusion

The energy problem in our planet is a challenge for the human being. Peter Glaser established the basis of a possible solution by introducing the space-based solar power concept. His idea has been the starting point of this project, although its final application differs.

An analysis of the design of a space-based thermosolar power satellite to provide 1.2 MW of energy to a future ISS has been done in this project. In addition, the regulatory frame and socio-economic context have been considered. The intention of this study was to propose a new possible way of power space stations and vehicles, assuming that in the future more energy than the one required nowadays would be needed.

The thermosolar power system that has been chosen for the satellite was a central tower one, which is composed by a cylindrical receiver placed in the top of the tower, a field of heliostats which concentrates sunlight into the receiver, and a Rankine cycle whose purpose is the conversion of solar radiation into electricity. Although each one of these elements have been designed individually along this project, they are all connected and the design of one part affects the others. In addition to the already mentioned components, in the present thesis it has been carried out an estimation of the accumulation system dimensions in order to produce energy continuously despite the presence of the eclipse periods.

A deeper analysis has been done in the design of the cylindrical receiver. The temperature profile of molten sodium as it passes through the panels and the exit temperature once all the path has been completed are the main design parameters that have been changed in order to select the one which better fulfilled the desired requirements. These changes have influenced the number of panels and thus the receiver dimensions.

After the developed study, some conclusions have been learned and possible improvements, identified. Some of the ways of improving the project are given

in Section 7.1, while Section 7.2 deals with the final conclusions.

## 7.1 Possible improvements for the project

The analysis performed in this project has been a very general one, although some important conclusions have been extracted. In this section, some points that may be improved are enumerated.

- For the sake of simplicity, the thermosolar power satellite has been designed maintaining the same configuration as a solar-thermal central receiver plant built on the ground. The lack of gravity has not been exploited as it could in this thesis, and a more efficient satellite could have been designed breaking the conventional distribution of elements and trying different structures as the ones shown in Figure 3.7.

- In the receiver design, just three basic temperature profiles where tested. If more research is done in that particular point, better results could be obtained and a more efficient receiver could be designed.

- Many of the values assumed in this project where just the typical ones. This is valid for a first approach, which was the intention of this project, but it could be improved for more detailed studies.

- It could have been also interesting to change some parameters in the Rankine cycle, and choose between different options as it was the case for the receiver. In addition, more complex Rankine cycles could be also tested, such as reheat cycles.

- Regarding the heliostat field, the layout used here is a relatively simple one. The problem could be optimized by using the advanced software tools that are already available in the industry.

## 7.2 Final conclusions

In the previous section it has been seen that there are many aspects which could be improved in the project. However, with the analysis performed on it, it is possible to get some conclusions.

As the project has been more focused on the design of the receiver, the most important conclusions that can be extracted deal with this element of the satellite.

From the three tested temperature profiles for sodium, it has been demonstrated

that the linear one is the best option, although a different selection criteria from the one used here could also be valid. On the other hand, the impossibility of having a logarithmic distribution has been proven.

Regarding the temperature at the outlet of the receiver, it has been concluded that the best option is a higher value. However, it is limited by the maximum temperature affordable by materials in order to maintain their properties.

When looking at the performances obtained for the power cycle, the receiver and the heliostat field, the feeling of having a very low efficiency arises and it is unavoidable to wonder whether thermal conversion system is really better than the photovoltaic one. Apart from the improvements that can be done in the analysis that would produce an increase in the plant performance, it must be always remembered that for the production of 1.2 MW, the efficiency of PV cells decreases. In addition, there are not yet any electric battery capable of storing such amount of power to overcome the eclipse periods, which cover a important fraction of the total orbit time. For these two reasons, the thermosolar satellite designed in this work is the best of the two options to power this possible future space station.

Finally, it could be said that acceptable results have been obtained for the thermosolar power satellite, and that, with the improvements that could already be done, it may be just a matter of time that this type of systems can be seen orbiting the Earth transforming sunlight into electric power.

# Bibliography


[1] E. Andrews, M. Baildon, E. Basinka, and J. Carll. Peter E. Glaser Papers. *MIT Libraries Archives* *http://libraries.mit.edu/archives*, 2004.

[2] Peter E. Glaser. Method and apparatus for converting solar radiation to electrical power. Patent., July 1971.

[3] A. Laverón and J. M. del Cura. Diseño, cálculo y certificación de vehículos aeroespaciales. Lecture notes (Univerisdad Politécnica de Madrid), 2015.

[4] ESA. International Space Station overview. *Available online:* *http://www.esa.int/esapub/br/br137/Br_137-1.pdf*, 1999.

[5] W. B. Stine and M. Geyer. *Power from the Sun.* Available online: http://www.powerfromthesun.net./book.html, 2001.

[6] Soteris Kalogirou. *Solar Energy Engineering: processes and systems.* Elsevier, 2009.

[7] J. Ignacio Ortega, J. Ignacio Burgaleta, and Félix M. Téllez. Central receiver system solar power plant using molten salt as heat transfer fluid. ASME, 2008.

[8] Isaac Asimov. *Reason.* Astounding Science Fiction, Street & Smith, 1941.

[9] DOE and NASA. Satellite power system concept development and evaluation program reference system report. Technical report, DOE and NASA, 1978.

[10] T. Wolsko, C. Brown, and R. Cirillo. *Preliminary assessment of the Satellite Power System (SPS) and six other energy technologies.* April 1980.

[11] John C. Mankins. Space Solar Power: The first international assesment of space solar power opportunities, issues and potential pathways forward. Technical report, International Academy of Astronautics, 2011.

[12] John C. Mankins. SPS-ALPHA: The First Practical Solar Power Satellite via Arbitrarily Large Phased Array. Technical report, NASA, 2012.

[13] Keith Henson. Thermal power satellites. *Online journal of space communication. Available online: https://spacejournal.ohio.edu*, 2015.

[14] Matthew J. Kleiman. Space law 101: An introduction to space law. *American Bar Association (ABA). Young Lawyers Division. Available online: https://www.americanbar.org/groups/young_lawyers*, 2010.

[15] United Nations Office for Outer Space Affairs. Space law. *Available online: http://www.unoosa.org/oosa/ourwork/spacelaw/*, 2014 [Accessed 7 September 2017].

[16] Keith Henson. Solving economics, energy, carbon and climate in a single project. *IEEE Conference on Technologies for Sustainability*, 2014.

[17] Isidoro Martínez. Spacecraft thermal control systems, missions and needs. Academic website: http://webserver.dmt.upm.es/~isidoro/, 2017.

[18] David G. Gilmore. *Spacecraft thermal control handbook. Volume I Fundamental technologies.* The Aerospace Corporation, 2002.

[19] Laboratory for Atmospheric and Space Physics. Equilibrium temperature. Available online: http://lasp.colorado.edu/home/, 2017.

[20] B. J. Anderson, C. G. Justus, and G. W. Batts. *Guidelines for the selection of near-Earth thermal environment parameters for spacecraft design.* NASA, 2001.

[21] Y. A. Çengel and M. A. Boles. *Thermodynamics. An Engineering Approach.* Mc Graw Hill Education, 2011.

[22] F. P. Incropera and D. P. De Witt. *Fundamentals of Heat and Mass Transfer.* John Wiley & Sons, 2007.

[23] J. K. Fink and L. Leibowitz. Thermodynamic and transport properties of sodium liquid and vapor. Technical report, Argonne National Laboratory, 1995.

[24] Miria M. Finckenor and Kim K. de Groh. International Space Station Researcher's Guide: Space Environmental Effects. Technical report, NASA, 2005.